Polarium model: Coherent radiation by a resonant medium

Sudhakar Prasad

Center for Advanced Studies and Department of Physics and Astronomy, University of New Mexico, Albuquerque, New Mexico 87131

Roy J. Glauber

Lyman Laboratory of Physics, Harvard University, Cambridge, Massachusetts 02138

In the absence of incoherent relaxation processes, the emission, absorption, and transport of resonant radiation by an extended medium are all cooperative processes in which the medium participates as a whole. Such radiative processes depend sensitively on the geometry of the source, on its size and density, and on the interplay of electric polarization resonances with the ambient electromagnetic field. By making a succession of simple approximations, we reduce the radiative interaction problem to one of solving a linear integral equation for the time-dependent polarization of the radiating medium. For the example of one-dimensional geometry, we show that the polarization possesses a sequence of exponentially decaying eigenmodes that oscillate at frequencies slightly shifted from that of the fundamental resonance. Only a few of these modes, for any radiating medium, are strongly coupled to the electromagnetic field, and thereby radiate efficiently. All of the other modes, infinitely many of them, are found to radiate quite slowly, or not at all. We consider in detail the radiation emitted by an arbitrary initial polarization distribution when the electromagnetic field is initially empty. Analytical and numerical results are presented for the time-dependent fields that follow from a wide variety of initial excitations. A locally oscillatory exchange of energy is found to take place between the electric and polarization fields, which gives rise to a ringing of the radiated intensity. The spectra of the emitted light are shown accordingly to be complex in structure, and to have a frequency gap which becomes independent of the size of the medium and its initial polarization distribution for media that are sufficiently large. The gap is caused by the interference and interaction of oppositely propagating excitations.

PACS number(s): 42.50.Fx, 42.50.Gy, 42.50.Md

I. INTRODUCTION

Most of the light we perceive is radiated, not by isolated atoms, but by atoms embedded in more or less extensive aggregates of other and similar atoms. The quantum radiated by a resonant excitation of any one of these atoms cannot travel any significant distance in such a medium before being absorbed and re-emitted by identical atoms situated nearby. The quantum tends thus to be trapped within the medium [1], and to make its way only slowly to the surface. This trapping of radiated quanta takes place both coherently and incoherently. It is the coherent aspect of the process that we address in the present paper. In this sense, the radiating elements are not individual atoms so much as the medium as a whole. The problem we address is thus the coupling of the entire atomic medium to the electromagnetic field. We find that by making suitable approximations we are able to treat a number of aspects of this daunting problem, and to predict some interesting features of the fields that are radiated.

Bulk matter abounds, of course, in properties that tend to break down the coherence of propagating waves. Random inhomogeneities of all sorts in a radiating medium tend to reduce its radiation to a state of incoherence. It is in the latter terms, as a problem of incoherent multiple scattering, that the larger question of radiation trapping has usually been addressed [2–7]. The effects of incoherence will surely tend to dilute, or perhaps even wash out, the various features that we find present in the coherent emission process, and we shall eventually have to address them. We have omitted them here, however, since the analysis must obviously begin with the coherent process. The descent from coherence into incoherence is irreversible, but may only be partial. It will be an interesting task for future work to see how much of the radiation process survives in a coherent form.

The process of coherent emission was discussed many years ago in its most elementary form by Dicke [8]. He pointed out that an aggregate of N atoms, lying within a volume small in dimension compared to the wavelength of light radiated, will only emit that radiation in somewhat unfamiliar ways. The excitations of the atoms can be described in terms of collective excitation modes, and it is only the symmetrical one among these that is appreciably coupled to the field. Any one of the atoms therefore can only radiate to the extent that it partakes in the symmetrical excitation. That is an effect of order $1/N$, so nearly all of its excitation energy remains trapped in that atom (until the much weaker effects of higher-order multipole couplings release it). The emission changes drastically when inhomogeneities are present, or nonradiative transitions are allowed to intervene. The excited atom may then radiate more or less independently of the others, and the quantum it radiates may then suffer successive scattering processes. What happens in realistic situations must surely combine and elaborate upon these contrasting images.

Our treatment of the coherent emission of radiation by matter is based upon three approximations. In the first of these, we assume that the atoms remain on the average close to their ground states. This is the assumption of weak excitation that embraces all of the familiar phenomena of linear optics. It implies that, with appropriate interpretation in

terms of coherent state amplitudes, much of our analysis can be carried out in essentially classical terms.

The second approximation we make is the smoothing of the discrete structure of the atomic medium. It is this smoothing that eliminates incoherent processes and treats matter as a continuous medium we shall call *polarium*. The polarization modes of this medium exchange energy with the electromagnetic field, but remain confined within finite boundaries. They therefore emit radiation freely at the boundaries, unlike the plane-wave modes that are often discussed for infinite media [9].

The third approximation we make is a simplification in treating the time dependence of the radiative interactions. We assume that all of the essential time dependences of the problem can be regarded as relatively slow modulations of an extremely rapid oscillation at the atomic resonance frequency ω_0. We assume further that light waves can cross the radiating medium in times much shorter than those in which the modulation takes place. It is important to understand that this rapid-transit approximation neglects only a small part of what are usually called retardation effects. As far as the rapid oscillations at the resonant frequency are concerned, retardation effects remain accounted for fully. The rapid transit approximation permits us to reduce the mathematical problem of treating the radiative interactions to an elementary form that can be solved analytically. It is a most convenient simplification, but it does place certain limits on the dimensions of the media we can treat. It is worth noting thus that the rapid transit approximation is the easiest of our three approximations to lift.

Each of the confined polarization modes we discuss decays exponentially with the emission of light. The decay periods are distributed, in general, over a broad range of values. Some of the modes for any medium are found to decay superradiantly, while the vast majority of them, an infinite number in fact, are found to radiate extremely slowly, or not at all. The decay of any given initial excitation, which may be expressed as a superposition of these modes, then proceeds according to a succession of different rates as the radiation of the faster modes precedes that of the slower ones. The exponential decay periods of the different modes are inevitably accompanied by certain shifts of the frequencies radiated. The total spectrum radiated thereby assumes a complex shape. It has a multipeaked structure that can contain sharply resonant dips as well. As the size of the medium increases, the spectrum develops a gap, representing frequencies at which propagation within the medium is strongly suppressed. Several of these features can be varied with the mode content of the initial polarization.

Our analysis bears a certain relation to one carried out many years ago by Burnham and Chiao [10] and then, in further detail, by others [11,12]. They studied the response of a semi-infinite medium of two-level atoms to a pulse of light incident upon it. The pulse was found to excite an oscillatory exchange of energy between the polarization of the medium and the electric field. This ringing phenomenon was actually observed in the tail of superradiant emission from an excited volume of gas atoms [13]. Analogous oscillatory exchanges of energy are present in the polarium model, which can ex-

hibit a much greater variety of ringing phenomena, according to the selection of modes excited.

Our paper begins with a discussion in Sec. II of the basic model of resonant medium-field coupling. We assume that the polarization of our atomic medium is initially different from zero, while the electromagnetic field begins in its vacuum state. Those assumptions are shown in Sec. III, where the rapid-transit approximation is introduced to define an initial value problem governed by a linear homogeneous integral equation. That equation is simplified in Sec. IV by assuming a slab geometry and excitations that are uniform in directions parallel to the slab faces. Under these conditions the problem is reduced to one dimension, and involves only scalar fields. A detailed discussion of the eigenvalue problem associated with our homogeneous linear integral equation, including its general features, certain exact sum rules, and approximate analytical and numerical expressions for the eigenvalues are presented in Sec. V. The exponentially decaying eigenmodes of the polarization can be superposed to express the solution of the general time-dependent problem in Sec. VI. There we also discuss the results of a more direct numerical solution of the integral equation, and illustrate the complex spectra radiated by a variety of initial excitations. We conclude that section with an approximate analytical treatment of the long-time behavior of a symmetric excitation that is initially very sharply localized. In Sec. VII, we address the problem of adding a frequency-independent susceptibility to the resonant one discussed in the prior sections, and show that it can be accounted for without complicating the mathematical methods introduced earlier. Some closing remarks are presented in Sec. VIII.

II. ATOM-FIELD INTERACTION

We consider a sample of N identical two-level atoms interacting with the electromagnetic field. The ground and excited states $|a\rangle$ and $|b\rangle$ have opposite parities, and are separated by energy $\hbar\omega_0$. We assume the wavelength $2\pi c/\omega_0$ is much larger than the atomic radius, so that the atoms interact with the electromagnetic field predominantly through electric dipole coupling. Furthermore, since the atoms differ only in their spatial locations $\vec{r}_i$, $i=1,\ldots,N$, it is sufficient to begin by discussing the interaction of a single atom with the field and then to generalize our equations to include all the atoms.

In the electric dipole approximation, the Hamiltonian H of an atom located at $\vec{r}$ interacting with the electromagnetic field takes the form

$$H = \frac{\hbar\omega_0}{2}\sigma_z - \vec{d}\cdot\vec{E}(\vec{r}) + H_F, \qquad (1)$$

in which σ_z is a familiar Pauli spin-1/2 operator, $\vec{d}$ is the atomic dipole moment operator, and H_F is the Hamiltonian of the free field. Since $\vec{d}$ is odd under spatial inversion and the two atomic states have opposite parities, the operator $\vec{d}$ may be expressed in terms of its vector matrix element $\vec{\mu} = \langle b|\vec{d}|a\rangle$ and the remaining Pauli spin operators $\sigma_\pm$ as

$$\vec{d}=\vec{d}_+ + \vec{d}_- \quad \text{with} \quad \vec{d}_+ = \vec{\mu}\sigma_+, \quad \vec{d}_- = \vec{\mu}^*\sigma_-. \quad (2)$$

The Pauli spin operators act on the atomic states as follows:

$$\sigma_+|a\rangle = |b\rangle, \quad \sigma_-|a\rangle = 0, \quad \sigma_z|a\rangle = -|a\rangle,$$

$$\sigma_+|b\rangle = 0, \quad \sigma_-|b\rangle = |a\rangle, \quad \sigma_z|b\rangle = |b\rangle,$$

and obey the familiar commutation rules

$$[\sigma_z,\sigma_\pm] = \pm 2\sigma_\pm, \quad [\sigma_+,\sigma_-] = \sigma_z.$$

When written in terms of $\vec{d}_\pm$ and the positive and negative frequency parts $\vec{E}^{(\pm)}(\vec{r})$ of the Hermitian electric field $\vec{E}$, the product $\vec{d}\cdot\vec{E}$ consists of four terms. We now make the rotating-wave approximation, which drops the two antiresonant terms $\vec{d}_+\cdot\vec{E}^{(-)}$ and $\vec{d}_-\cdot\vec{E}^{(+)}$, but retains and correctly treats the resonant and near-resonant interactions $\vec{d}_+\cdot\vec{E}^{(+)}$ and $\vec{d}_-\cdot\vec{E}^{(-)}$ that characterize the standard treatments of radiation damping. The effective Hamiltonian is then

$$H = \frac{\hbar\omega_0}{2}\sigma_z - \{\sigma_+[\vec{\mu}\cdot\vec{E}^{(+)}(\vec{r})] + \sigma_-[\vec{\mu}^*\cdot\vec{E}^{(-)}(\vec{r})]\} + H_F. \quad (1')$$

Application of the commutation rules to this Hamiltonian yields the Heisenberg equation of motion for the dipole operator $\vec{d}_-$:

$$\frac{d}{dt}\vec{d}_- = -i\omega_0\vec{d}_- - i\frac{\vec{\mu}^*}{\hbar}[\vec{\mu}\cdot\vec{E}^{(+)}(\vec{r},t)]\sigma_z. \quad (3)$$

The further equations of motion couple the time derivative of the operator σ_z in turn to the $\sigma_\pm$ operators, but we need not construct them here since all the phenomena we propose to discuss can be described in terms of weak atomic excitations. We thus assume that the atom is never far from its ground state $|a\rangle$ and that σ_z in Eq. (3) can be replaced approximately by its eigenvalue -1, so that

$$\frac{d}{dt}\vec{d}_- = -i\omega_0\vec{d}_- + i\frac{\vec{\mu}^*}{\hbar}[\vec{\mu}\cdot\vec{E}^{(+)}(\vec{r},t)]. \quad (4)$$

This linearization of the equation of motion is equivalent to replacing the two-level atom by a harmonic oscillator of frequency ω_0, an approximation that remains accurate as long as the occupation probabilities for the states of quantum number $n\geq 1$ remain negligible. While the compass of this linearized model is not without restrictions, its range of validity does include virtually all the phenomena of ordinary or linear optics, i.e., refraction, reflection, scattering, radiation damping, etc.

Restricting our considerations to weak excitations of individual atoms or oscillators will not stand in the way of our macroscopically treating measurable polarization fields, once we take into account the large number of atoms in our sample. Equation (4) has been derived, strictly speaking, as a relation between the polarization operator $\vec{d}(t)$ and the field

operator $\vec{E}^{(+)}(\vec{r},t)$ in the Heisenberg picture, but, since it is linear, it may be regarded equally well as a relation between the expectation values of these operators, and in that sense it furnishes a classical equation as well.

The reason the classical and quantum-mechanical treatments correspond so closely is that the electromagnetic field behaves as an ensemble of harmonic oscillators while, as we have noted earlier, weakly excited atoms can also be represented by harmonic oscillators. The special coupling between these oscillators described by our equations of motion is of a type [14] that always carries coherent states of the system into new coherent states in the time-dependent Schrödinger picture. Furthermore, the amplitudes of those coherent states simply obey the classical equations of motion. In this sense, then, there is no loss of generality in solving just the classical equations. All quantum fluctuations can be found, for example, by using the classical solutions to construct the appropriate coherent states.

Let us now define a microscopic polarization density operator for the collection of point dipoles, and separate it into its positive and negative frequency parts, $\vec{P}(\vec{r},t) = \vec{P}^{(+)}(\vec{r},t) + \vec{P}^{(-)}(\vec{r},t)$, so that

$$\vec{P}^{(+)}(\vec{r},t) = \sum_{i=1}^N \vec{d}_-^{(i)}(t)\,\delta(\vec{r}-\vec{r}_i) = [\vec{P}^{(-)}(\vec{r},t)]^\dagger, \quad (5)$$

where $\vec{d}_-^{(i)}$ is the dipole moment operator for the ith atom. By appending the label i to $\vec{d}_-$, $\vec{\mu}$, and $\vec{r}$ in Eq. (4), multiplying the resulting equation by $\delta(\vec{r}-\vec{r}_i)$, and then summing over all $i=1,\ldots,N$, we obtain the equation of motion for the microscopic polarization density $\vec{P}^{(+)}(\vec{r},t)$,

$$\left(\frac{\partial}{\partial t}+i\omega_0\right)\vec{P}^{(+)}(\vec{r},t) = \frac{i}{\hbar}\mathbf{M}(\vec{r})\cdot\vec{E}^{(+)}(\vec{r},t), \quad (6)$$

in which $\mathbf{M}(\vec{r})$ is a second-rank tensor with the following dyadic form:

$$\mathbf{M}(\vec{r}) = \sum_{i=1}^N \vec{\mu}_i^*\vec{\mu}_i\delta(\vec{r}-\vec{r}_i). \quad (7)$$

While Eq. (6) describes how the polarization density is influenced by the electromagnetic field, the field responds in turn to the polarization density via the Maxwell wave equation

$$-\vec{\nabla}\times(\vec{\nabla}\times\vec{E}^{(+)}) - \frac{1}{c^2}\frac{\partial^2}{\partial t^2}\vec{E}^{(+)} = \frac{1}{c^2}\frac{\partial^2}{\partial t^2}\vec{P}^{(+)}. \quad (8)$$

We have, to this point, retained the microscopic picture of the polarization density and the electric field that is implicit in the singular expressions (6) and (8). The atomic medium we shall be concerned with, however, will be essentially continuous in nature, and so we will treat both $\vec{P}(\vec{r},t)$ and $\vec{E}(\vec{r},t)$ as continuous functions of $\vec{r}$. Mathematically, the required smoothing is accomplished by averaging Eqs. (6) and

(8) over volumes large enough to contain many atomic dipoles, but still much smaller in their dimensions than the wavelength $2\pi/k_0$. We shall assume, furthermore, that the atomic medium is isotropic, so that its electric polarization is always parallel to the inducing field. That will be so in our two-state model as long as the dipole matrix-element vectors of the atoms within any smoothing volume are randomly oriented. When they are distributed thus and averaged over, the dyadic function $\mathbf{M}(\vec{r})$ reduces to the unit dyadic multiplied by $(|\vec{\mu}|^2/3)n(\vec{r})$, where $n(\vec{r})$ is the smoothed number density function. Thus Eq. (6) reduces to the simpler form

$$\left(\frac{\partial}{\partial t}+i\omega_0\right)\vec{P}^{(+)}(\vec{r},t)=i\frac{|\vec{\mu}|^2}{3\hbar}n(\vec{r})\vec{E}^{(+)}(\vec{r},t). \quad (9)$$

In deriving Eq. (9), we have implicitly ignored local field effects by assuming that the electric field acting on each atom is the same as the averaged field $\vec{E}^{(+)}(\vec{r},t)$. In fact, in a familiar approximation [15], the local field can be written in terms of the smoothed fields as $\vec{E}^{(+)}(\vec{r},t)+(1/3)\vec{P}^{(+)}(\vec{r},t)$. The effect of that correction in a uniform medium is then equivalent to a downward shift of the resonant frequency,

$$\Delta\omega=-\frac{n_0|\vec{\mu}|^2}{9\hbar}.$$

If we redefine ω_0 to include this correction, we may retain Eq. (9) as shown.

The derivation of Eq. (9) has also assumed that the smoothed product $\mathbf{M}(\vec{r})\cdot\vec{E}(\vec{r},t)$ in Eq. (6) is well approximated by the product of the smoothed functions $\mathbf{M}(\vec{r})$ and $\vec{E}(\vec{r},t)$. By doing this, we have postponed consideration of certain density fluctuation effects that typically lead to incoherent scattering. We shall refer to this idealized model of a continuous, isotropic, polarizable medium as *polarium*.

Since Eq. (9) will play a fundamental role in our analysis, we should note that it holds for atomic models considerably more realistic than the elementary two-state model we have used to derive it. A more direct way of achieving isotropy, for example, is to let each atom respond isotropically. The atomic ground states might thus be *s* states, and the excited states three degenerate *p* states. In this four-state model we likewise secure a relation between $\vec{P}^{(+)}$ and $\vec{E}^{(+)}$ similar to Eq. (9), but with $|\vec{\mu}|^2/3$ replaced by the squared matrix element connecting the *s* state to any of the three *p* states [16].

For the geometrically simple problems that we shall consider in the present paper, the smoothed electric field and polarization will be purely transverse fields:

$$\vec{\nabla}\cdot\vec{P}^{(+)}(\vec{r},t)=0,\quad\vec{\nabla}\cdot\vec{E}^{(+)}(\vec{r},t)=0.$$

In that case, all of the terms in Eq. (8) are transverse, and it reduces to the form

$$\left(\nabla^2-\frac{1}{c^2}\frac{\partial^2}{\partial t^2}\right)\vec{E}^{(+)}(\vec{r},t)=\frac{1}{c^2}\frac{\partial^2}{\partial t^2}\vec{P}^{(+)}(\vec{r},t). \quad (10)$$

When we deal with other geometries in later work, we shall have to return to Eq. (8) and treat the longitudinal field components more explicitly.

It is worth emphasizing that we have only treated the resonant interaction of a single atomic transition with the electromagnetic field. The atoms we are considering will typically have many spectral resonances at other frequencies. Any other atoms that are present in the medium will add further contributions to the polarization density. If we restrict our consideration to a narrow enough spectral interval around ω_0, the contributions of other resonances and other atoms can be treated as a frequency-independent background susceptibility to be added to the resonant susceptibility implicit in our calculations. This modification of the treatment of our central problem, that of the resonant interaction, is introduced in Sec. VII.

III. AN INITIAL VALUE PROBLEM
FOR THE POLARIZATION

The physical problem we shall consider first concerns the way in which an initial excitation of the atomic sample evolves and propagates under interaction with the electromagnetic field. We shall take the electric field to begin in its vacuum state. Any vacuum fluctuations that are present initially induce a random polarization background and do not contribute to the expectation values of the polarization or to any of its normally ordered moments. Since these are the only moments we need to calculate, we may in effect ignore the zero-point field. For this problem, Eq. (10) can be conveniently cast into an integral form by making use of the retarded potential

$$\vec{E}^{(+)}(\vec{r},t)=-\frac{1}{c^2}\int\frac{\partial^2}{\partial t'^2}\vec{P}^{(+)}(\vec{r}',t')$$

$$\times\frac{\delta\left(t-t'-\frac{|\vec{r}-\vec{r}'|}{c}\right)}{4\pi|\vec{r}-\vec{r}'|}d\vec{r}'dt'$$

$$=-\frac{1}{c^2}\int\frac{\frac{\partial^2}{\partial t^2}\widetilde{P}^{(+)}\left(\vec{r}',t-\frac{|\vec{r}-\vec{r}'|}{c}\right)}{4\pi|\vec{r}-\vec{r}'|}d\vec{r}'. \quad (11)$$

By expressing $\vec{E}^{(+)}$ and $\vec{P}^{(+)}$ in terms of their slowly varying envelopes $\vec{\mathcal{E}}$ and $\vec{\mathcal{P}}$,

$$\vec{E}^{(+)}(\vec{r},t)=\vec{\mathcal{E}}(\vec{r},t)e^{-i\omega_0 t},\quad\vec{P}^{(+)}(\vec{r},t)=\vec{\mathcal{P}}(\vec{r},t)e^{-i\omega_0 t}, \quad (12)$$

and dropping the relatively small time derivatives of $\vec{\mathcal{P}}$, we may reduce Eq. (11) to the form

$$\vec{\mathcal{E}}(\vec{r},t)=k_0^2\int\mathcal{P}\left(\vec{r}',t-\frac{|\vec{r}-\vec{r}'|}{c}\right)\frac{e^{ik_0|\vec{r}-\vec{r}'|}}{4\pi|\vec{r}-\vec{r}'|}d\vec{r}'. \quad (13)$$

The use of the envelopes (12) in Eq. (6) leads to the equation of motion for the polarization:

$$\frac{\partial}{\partial t}\vec{\mathcal{P}}(\vec{r},t)=i\frac{|\vec{\mu}|^2}{3\hbar}n(\vec{r})\vec{\mathcal{E}}(\vec{r},t). \quad (14)$$

We shall take Eqs. (13) and (14) to be fundamental in the work that follows. The density $n(\vec{r})$, and therefore the polarization $\vec{\mathcal{P}}(\vec{r},t)$, we shall assume, both vanish outside some restricted volume V. An interesting initial value problem is one in which the polarization $\vec{\mathcal{P}}(\vec{r},0)$ at time $t=0$ takes on a given value within some subvolume of V, while the electric field, as noted earlier, vanishes everywhere at $t=0$. We use the equations of motion to investigate the spreading and ultimate decay of the polarization within the medium, and to discuss the electric field that is generated and eventually radiated. It is clear from Eq. (13) that the electric field $\vec{\mathcal{E}}(\vec{r},t)$ must obey an outgoing wave boundary condition at the surface of the volume V; Eq. (14) shows that the polarization must also satisfy an outgoing wave boundary condition in the surface region.

When we substitute the expression given by Eq. (13) for the electric field amplitude into Eq. (14), we secure a single equation for the polarization amplitude:

$$\frac{\partial}{\partial t}\vec{\mathcal{P}}(\vec{r},t)=i\frac{|\vec{\mu}|^2n(\vec{r})k_0^2}{3\hbar}\int\frac{e^{ik_0|\vec{r}-\vec{r}'|}}{4\pi|\vec{r}-\vec{r}'|}\vec{\mathcal{P}}\left(\vec{r}',t-\frac{|\vec{r}-\vec{r}'|}{c}\right)d\vec{r}'. \quad (15)$$

It is worth emphasizing that the polarization amplitude described by Eq. (15) is the slowly varying envelope function defined by Eq. (12). The integrand on the right side of Eq. (15) requires evaluating the function $\vec{\mathcal{P}}$ at the retarded time $t-|\vec{r}-\vec{r}'|/c$, but if its temporal variation is sufficiently slow a good approximation may be achieved by neglecting the retardation in $\vec{\mathcal{P}}$ and writing

$$\frac{\partial}{\partial t}\vec{\mathcal{P}}(\vec{r},t)=i\frac{|\vec{\mu}|^2n(\vec{r})k_0^2}{3\hbar}\int\frac{e^{ik_0|\vec{r}-\vec{r}'|}}{4\pi|\vec{r}-\vec{r}'|}\vec{\mathcal{P}}(\vec{r}',t)d\vec{r}'. \quad (16)$$

This equation, as we shall see, is a convenient one to solve as an initial value problem. By approximating only the slowly varying envelope, furthermore, it omits, in general, only a small part of the overall effect of retardation. The larger part of that effect, represented by the rapidly oscillating factor in the polarization of Eq. (12), is still accounted for by the factor $\exp(ik_0|\vec{r}-\vec{r}'|)$ present in the integrand of Eq. (16). The assumption underlying Eq. (16), which we shall call the rapid-transit approximation, will clearly be a good one as long as the envelope function $\vec{\mathcal{P}}$ varies slowly enough in time, and that, as we shall see, is often the case. Of course, any such approximation will tend to place limits on how large the system can be, and we shall address them in detail in Sec. V. We shall show that there is ample room within these constraints to observe many physically interest-ing behaviors of both the polarization and the electric field. To discuss the problem further, we shall have to solve Eq. (16).

IV. REDUCTION TO ONE DIMENSION

We shall undertake the solution of Eq. (16) as a three-dimensional problem in later work. It will be most helpful here to consider an essentially one-dimensional version of the problem it poses. Let us assume that the atomic medium has a uniform density n_0 within the bounds $-L/2\leq z\leq L/2$, and that its extent in the transverse directions x and y is unbounded. The polarization amplitude, we assume, depends only on z and t, and must vanish for $|z|>L/2$.

To carry out the reduction of Eq. (16), we write the coordinate vectors $\vec{r}$ and $\vec{r}'$ in terms of their transverse and longitudinal components as $\vec{r}=(\vec{\rho},z)$ and $\vec{r}'=(\vec{\rho}',z')$, and let $\vec{\rho}''=\vec{\rho}'-\vec{\rho}$ and $s=[\rho''^2+(z'-z)^2]^{1/2}$. Then Eq. (16) becomes

$$\frac{\partial}{\partial t}\vec{\mathcal{P}}(z,t)=i\frac{|\vec{\mu}|^2n_0k_0^2}{3\hbar}\int_{-L/2}^{L/2}\vec{\mathcal{P}}(z',t)dz'\int_{|z-z'|}^{\infty}\frac{e^{ik_0s}}{4\pi s}2\pi sds.$$

We may, at this stage, suppress the vector character of the polarization amplitude $\vec{\mathcal{P}}$ by noting that the two independent, transverse components of $\vec{\mathcal{P}}$ obey the same equation, a fact that leads merely to a twofold degeneracy of the characteristic solutions of our initial-value problem. The integration over the variable s is elementary, but the oscillating contribution of its upper limit remains ambiguous. This contribution can be taken to vanish either by giving to k_0 an infinitesimal positive imaginary part, or alternatively by breaking slightly the invariance of $\mathcal{P}$ under transverse displacements to allow for an infinitesimally slow decrease of $\mathcal{P}(\vec{r},t)$ as $\rho\rightarrow\infty$. In either case, the equation for the polarization in one dimension reduces to

$$\frac{\partial}{\partial t}\mathcal{P}(z,t)=-\frac{|\vec{\mu}|^2n_0k_0}{6\hbar}\int_{-L/2}^{L/2}\mathcal{P}(z',t)e^{ik_0|z-z'|}dz' \quad (17)$$

for $|z|\leq L/2$. The corresponding value of the electric field $\mathcal{E}(z,t)$ is given as

$$\mathcal{E}(z,t)=\frac{ik_0}{2}\int_{-L/2}^{L/2}\mathcal{P}(z',t)e^{ik_0|z-z'|}dz'. \quad (18)$$

It is convenient to reduce Eq. (17) to a form involving only scaled space and time coordinates by introducing the variables Z and T,

$$Z=\frac{z}{L}, \quad T=\frac{t}{\tau_R}, \quad (19)$$

where

$$\frac{1}{\tau_R}\equiv\frac{n_0\vec{\mu}|^2\beta}{6\hbar} \quad \text{with} \quad \beta\equiv k_0L. \quad (20)$$

The quantity $1/\tau_R$ is essentially the Dicke superradiance rate defined by Arecchi and Courtens [17], and we shall discuss it further in Sec. V.

In these scaled units, Eq. (17) reduces to the form

$$\frac{\partial}{\partial T}\mathcal{P}(Z,T)=-\int_{-1/2}^{1/2}dZ'\,e^{i\beta|Z-Z'|}\mathcal{P}(Z',T),\quad |Z|\leq 1/2,$$
(21)

in which the only surviving parameter is β, the sample thickness measured in units of the reduced wavelength $1/k_0$.

As we have noted earlier, in the absence of any initial electric field, only outgoing polarization waves can exist at the boundaries of the medium, $Z=\pm 1/2$. These waves support an outflow of energy that is irretrievably lost from the medium as electromagnetic radiation. That the polarization energy can only decrease is directly implied by Eq. (21). To see this, we multiply Eq. (21) by $\mathcal{P}^*(Z,T)$, and consider the real part of the resulting equation:

$$\frac{\partial}{\partial T}[|\mathcal{P}(Z,T)|^2]=-\int_{-1/2}^{1/2}dZ'[e^{i\beta|Z-Z'|}\mathcal{P}(Z',T)\mathcal{P}^*(Z,T)$$
$$+e^{-i\beta|Z-Z'|}\mathcal{P}^*(Z',T)\mathcal{P}(Z,T)].$$

By integrating this equation over Z, we obtain an equation that describes the rate of change of polarization energy in the volume V:

$$\frac{d}{dT}\left[\int_{-1/2}^{1/2}|\mathcal{P}(Z,T)|^2 dZ\right]$$

$$=-\int_{-1/2}^{1/2}dZ\int_{-1/2}^{1/2}dZ'[e^{i\beta|Z-Z'|}\mathcal{P}(Z',T)\mathcal{P}^*(Z,T)$$
$$+e^{-i\beta|Z-Z'|}\mathcal{P}^*(Z',T)\mathcal{P}(Z,T)].$$

The variables Z and Z' may be freely interchanged in the second term of the integrand, with the result

$$\frac{d}{dT}\left[\int_{-1/2}^{1/2}|\mathcal{P}(Z,T)|^2 dZ\right]$$

$$=-2\int_{-1/2}^{1/2}dZ\int_{-1/2}^{1/2}dZ'\cos(\beta|Z-Z'|)$$
$$\times\mathcal{P}(Z',T)\mathcal{P}^*(Z,T).$$

Since $\cos\beta|Z-Z'|=\cos\beta Z\cos\beta Z'+\sin\beta Z\sin\beta Z'$, the double integral may be reduced to an explicitly positive-definite form, so that we find

$$\frac{d}{dT}\left[\frac{1}{2}\int_{-1/2}^{1/2}|\mathcal{P}(Z,T)|^2 dZ\right]$$

$$=-\left[\left|\int_{-1/2}^{1/2}dZ\mathcal{P}(Z,T)\cos\beta Z\right|^2\right.$$
$$+\left.\left|\int_{-1/2}^{1/2}dZ\mathcal{P}(Z,T)\sin\beta Z\right|^2\right]\leq 0.$$
(22)

In other words, the total polarization energy stored in the medium can only decay with time as a result of interaction with the electric field.

V. ONE-DIMENSIONAL EIGENVALUE PROBLEM

The task of solving Eq. (21) is simplified greatly by the separability of its dependences on Z and T. In particular, if we seek solutions of the form $e^{-\lambda T}P_\lambda(Z)$, then $P_\lambda(Z)$ must satisfy the homogeneous Fredholm integral equation

$$\lambda P_\lambda(Z)=\int_{-1/2}^{1/2}dZ'\,e^{i\beta|Z-Z'|}P_\lambda(Z').$$
(23)

This equation defines an eigenvalue problem for which the relation (22) assures us that all the eigenvalues will have non-negative real parts, $\mathrm{Re}(\lambda)\geq 0$. The boundary conditions implicit in Eq. (23) are the outgoing-wave conditions

$$P_\lambda(Z)\to e^{i\beta|Z|}\times\mathrm{const}\quad\text{for }|Z|\to\tfrac{1}{2},$$
(24)

and these, as we shall see, restrict the eigenvalues to a discrete sequence.

Many of the important properties of the functions $P_\lambda(Z)$ and the eigenvalues λ follow simply from the general structure of Eq. (23). It will be useful to demonstrate several of them before undertaking an explicit solution of the equation. Let $P_{\lambda'}(Z)$ be an eigenfunction of Eq. (23) corresponding to the eigenvalue $\lambda'\neq\lambda$. Then it obeys

$$\lambda'P_{\lambda'}(Z)=\int_{-1/2}^{1/2}dZ'\,e^{i\beta|Z-Z'|}P_{\lambda'}(Z').$$
(25)

Now if we multiply Eq. (23) by $P_{\lambda'}(Z)$ and Eq. (25) by $P_\lambda(Z)$, take the difference of the two equations, and then integrate over Z, we find

$$(\lambda-\lambda')\int_{-1/2}^{1/2}P_\lambda(Z)P_{\lambda'}(Z)dZ$$

$$=\int_{-1/2}^{1/2}dZ\int_{-1/2}^{1/2}dZ'\,e^{i\beta|Z-Z'|}$$
$$\times[P_\lambda(Z')P_{\lambda'}(Z)-P_\lambda(Z)P_{\lambda'}(Z')].$$

Interchange of the integration variables Z and Z' in the integrand on the right shows that the integral vanishes. It follows then that for $\lambda\neq\lambda'$, the two solutions $P_\lambda(Z)$ and $P_{\lambda'}(Z)$ are orthogonal:

$$\int_{-1/2}^{1/2} P_\lambda(Z)P_{\lambda'}(Z)dZ=0 \quad (\lambda \neq \lambda'). \qquad (26)$$

The eigenfunctions can be given unit normalization, so that the general orthonormality relation is obtained:

$$\int_{-1/2}^{1/2} P_\lambda(Z)P_{\lambda'}(Z)dZ=\delta_{\lambda,\lambda'}. \qquad (27)$$

The kernel function $\exp(i\beta|Z-Z'|)$ is symmetric under spatial inversion $Z\rightarrow -Z$ and $Z'\rightarrow -Z'$, as is the medium itself. It follows that if $P_\lambda(Z)$ is a solution of Eq. (23), then $P_\lambda(-Z)$ is also a solution corresponding to the same eigenvalue λ. We shall show presently that the eigenvalues in the one-dimensional problem are, in general, nondegenerate. Hence $P_\lambda(Z)$ and $P_\lambda(-Z)$ can only differ by a constant factor, and that factor can only be ± 1. The eigenfunctions $P_\lambda(Z)$ are thus either even or odd functions of Z.

From the general theory of Hilbert-Schmidt symmetric kernels [18], it follows that the eigenfunctions $P_\lambda(Z)$ form a complete set on the interval $-1/2 \leq Z \leq 1/2$. Thus we can expand the kernel function $\exp(i\beta|Z-Z'|)$ in terms of the P_λ as

$$e^{i\beta|Z-Z'|}=\sum_\lambda c_\lambda(Z)P_\lambda(Z'),$$

where the expansion coefficient $c_\lambda(Z)$ is given by

$$c_\lambda(Z)=\int_{-1/2}^{1/2} e^{i\beta|Z-Z'|}P_\lambda(Z')dZ'=\lambda P_\lambda(Z).$$

The kernel thus possesses the expansion

$$e^{i\beta|Z-Z'|}=\sum_\lambda \lambda P_\lambda(Z)P_\lambda(Z'). \qquad (28)$$

An immediate application of this relation is obtained by letting $Z'=Z$ and integrating over Z from $-1/2$ to $1/2$. The result is a sum rule showing that the eigenvalues all add up to unity,

$$\sum_\lambda \lambda=1. \qquad (29)$$

Since the eigenvalues are complex, this relation amounts to two sum rules

$$\sum_\lambda \mathrm{Re}\,\lambda=1, \quad \sum_\lambda \mathrm{Im}\,\lambda=0. \qquad (30)$$

There are a number of other sum rules that follow from the expansion in Eq. (28). These concern sums of powers of the eigenvalues λ and partial sums of eigenvalues taken over the even and odd solutions. These sum rules are derived in Appendix A.

A. Radiation by a thin slab, $\beta \ll 1$

A helpful introductory problem, and the simplest one to discuss, is the limiting case in which the slab thickness L is much smaller than the reduced wavelength $\lambdabar_0=1/k_0$. For $\beta=k_0L\ll 1$ we see that Eq. (23) reduces to

$$\lambda P_\lambda(Z)\approx \int_{-1/2}^{1/2} P_\lambda(Z')dZ'. \qquad (31)$$

If we integrate both sides of this equation from $-1/2$ to $1/2$, we find

$$(\lambda-1)\int_{-1/2}^{1/2} P_\lambda(Z')dZ'=0,$$

a relation that can only be obeyed if either $\lambda=1$ or, alternatively,

$$\int_{-1/2}^{1/2} P_\lambda(Z)dZ=0. \qquad (32)$$

If $\lambda=1$, then according to Eq. (31) the polarization must be uniform over the volume of the slab. Otherwise Eq. (32) must hold and the polarization averages to zero. All polarization modes of this character, according to Eq. (31), must have $\lambda=0$. The thin slab then represents a limiting case in which there is a single fundamental mode with $\lambda=1$, and a sequence of spatially oscillating modes with the common eigenvalue $\lambda=0$. The eigenvalue $\lambda=1$ for the fundamental uniform mode corresponds to a decay period for the polarization of $\tau_R=6\hbar/(n_0|\vec{\mu}|^2k_0L)=6\hbar/(n_0|\vec{\mu}|^2\beta)$.

The remaining modes with $\lambda=0$ clearly do not decay at all. It is not difficult to see why that should be so if we refer back to Eq. (18) for the electric field. In scaled form it is

$$\mathcal{E}(Z,T)=\frac{i\beta}{2}\int_{-1/2}^{1/2}\mathcal{P}(Z',T)e^{i\beta|Z-Z'|}dZ', \qquad (33)$$

and for $\beta \ll 1$ it reduces within the slab to

$$\mathcal{E}(Z,T)=\frac{i\beta}{2}\int_{-1/2}^{1/2}\mathcal{P}(Z',T)dZ'. \qquad (34)$$

The contribution of any eigenfunction P_λ to the field can then be written as

$$\mathcal{E}_\lambda(Z,T)=\frac{i\beta}{2}\int_{-1/2}^{1/2}P_\lambda(Z')dZ'e^{-\lambda T}. \qquad (35)$$

The polarization modes with eigenvalue $\lambda=0$ are inhibited in their decay because for them the polarization integrals in Eq. (35) all vanish. Their polarization energy remains trapped within the slab in the limit $k_0L\ll 1$ because their mode functions are orthogonal to the electric field waves of frequency ω_0. The latter waves are nearly uniform within the thin slab.

The fundamental mode for the polarization which is spatially uniform is the only one that radiates efficiently for a thin slab. Its decay rate in unscaled physical units is

$$\tau_R^{-1} = \frac{n_0 |\vec{\mu}|^2 k_0 L}{6\hbar}. \tag{36}$$

We can see in the proportionality of this number to $n_0 L$, the number of atoms per unit area of the slab, that the radiation process, viewed from an atomic standpoint, must be a cooperative one. The radiative decay rate for a single free atom is

$$\tau^{-1} = \frac{|\vec{\mu}|^2 k_0^3}{6\pi\hbar}. \tag{37}$$

The decay rate τ_R^{-1} is enhanced over τ^{-1} by a factor of order $n_0 L / k_0^2$, which we must assume to be larger than unity in order to have the right to consider the slab as a continuous medium. There must, in other words, be more than one atom in the slab per square wavelength on the average. The atoms within each such area then radiate cooperatively in the $\pm z$ directions through mutual interference.

We can explain the enhancement factor $n_0 L / k_0^2$ from a more dynamical viewpoint by taking the thin slab to be large but finite in its lateral dimensions. If it has area A, then it contains $N = n_0 A L$ atoms. The enhancement factor can thus be written as

$$\frac{n_0 L}{k_0^2} = N \frac{1}{k_0^2 A}. \tag{38}$$

The rate of decay of the excitation of any atom in the slab is increased by the Dicke superradiance factor $N/4$ since all of the atoms in the slab radiate coherently. The decay rate is decreased, on the other hand, because each atom can only radiate into a solid angle [17] smaller than 4π by a factor of order $(k_0^2 A)^{-1}$. That inhibition, on the radiation by any one atom, is another feature of the cooperative effect of all the other atoms radiating in the same phase.

B. Solution for the eigenfunctions and eigenvalues

The solutions to Eq. (23) merit careful attention since, as we shall later see, they also occur in three-dimensional problems defined in spherical volumes. The Fredholm equation (23) is a particularly simple one to solve since it can be reduced to a familiar differential equation. To accomplish that reduction, we need only observe that the kernel $\exp(i\beta|Z-Z'|)$ is the Green's function of the differential operator $\partial^2/\partial Z^2 + \beta^2$, i.e., that

$$\left(\frac{\partial^2}{\partial Z^2} + \beta^2\right) e^{i\beta|Z-Z'|} = 2i\beta\delta(Z-Z'). \tag{39}$$

When we apply the differential operator to both sides of Eq. (23) we see that $P_\lambda(Z)$ must satisfy the differential equation

$$\left(\frac{\partial^2}{\partial Z^2} + \beta^2 - \frac{2i\beta}{\lambda}\right) P_\lambda(Z) = 0, \tag{40}$$

for $-1/2 \leq Z \leq 1/2$.

The electric-field amplitude $\mathcal{E}_\lambda(Z)$ that corresponds to the polarization mode $P_\lambda(Z)$ is simply proportional to $P_\lambda(Z)$

according to Eq. (14). It therefore satisfies the same differential equation as $P_\lambda(Z)$ for $-1/2 \leq Z \leq 1/2$. For $|Z| > 1/2$, on the other hand, it obeys the free-wave equation

$$\left(\frac{\partial^2}{\partial Z^2} + \beta^2\right) \mathcal{E}_\lambda(Z) = 0. \tag{41}$$

The electric-field amplitude $\mathcal{E}_\lambda(Z)$ thus satisfies a species of stationary-state Schrödinger equation for a particle of positive energy proportional to β^2, but interacting with a complex "square-well" potential. Because the imaginary part of the potential is positive, the polarizations $P_\lambda(Z)$ tend to be amplified spatially with increasing $|Z|$.

It is convenient to define a complex parameter,

$$\gamma_\lambda = \sqrt{\beta^2 - \frac{2i\beta}{\lambda}}, \tag{42}$$

so that Eq. (40) can be written more compactly as

$$\left(\frac{d^2}{dZ^2} + \gamma_\lambda^2\right) P_\lambda(Z) = 0, \tag{43}$$

and the quantity γ_λ/L plays the role of a complex propagation constant. The even solutions, normalized according to Eq. (27), then take the form

$$P_\lambda^{(e)}(Z) = \sqrt{\frac{2}{1 + \frac{\sin\gamma_\lambda}{\gamma_\lambda}}} \cos\gamma_\lambda Z. \tag{44}$$

Their logarithmic derivatives must match those of $\exp(i\beta|Z|)$ at the boundaries $Z = \pm 1/2$, and these conditions are met provided that

$$-\gamma_\lambda \tan\left(\frac{\gamma_\lambda}{2}\right) = i\beta. \tag{45}$$

The odd solutions to Eq. (43) may be obtained by similar means. They take the form

$$P_\lambda^{(o)}(Z) = \sqrt{\frac{2}{1 - \frac{\sin\gamma_\lambda}{\gamma_\lambda}}} \sin\gamma_\lambda Z, \tag{46}$$

where the outgoing-wave boundary conditions at $Z = \pm 1/2$ require γ_λ to satisfy the relation

$$\gamma_\lambda \cot\left(\frac{\gamma_\lambda}{2}\right) = i\beta. \tag{47}$$

Because the tangent and cotangent functions each have an infinite set of discrete branches, the eigenvalue conditions (45) and (47) restrict the permissible values of λ to two discrete, infinite, nondegenerate sets via the relation inverse to Eq. (42):

$$\lambda = \frac{2i\beta}{\beta^2 - \gamma_\lambda^2}. \tag{48}$$

The two sets of eigenvalues cannot have any common elements, however, since then Eqs. (45) and (47) would lead to the contradiction

$$\sin^2\frac{\gamma_\lambda}{2} + \cos^2\frac{\gamma_\lambda}{2} = 0.$$

The real part of any such eigenvalue represents the decay rate of the associated mode, while its imaginary part represents a shift of the oscillation frequency of the mode from the medium resonance ω_0. The precise values of the eigenvalue roots of Eqs. (45) and (47) can only be found in general by numerical means. It is possible to approximate the roots analytically, however, for all values of β and for broad ranges of the complex λ plane.

C. Approximate expressions for the eigenvalues

Although exact closed-form expressions cannot be obtained for the eigenvalues, relations (45) and (46) permit approximate perturbative solutions in certain limits.

For a vanishingly thin medium, as we saw earlier, there are only two eigenvalues possible; $\lambda=1$ for the fundamental superradiant mode, and $\lambda=0$ for all other, nondecaying modes. With increasing medium thickness, although still with $\beta\ll1$, the fundamental eigenvalue develops an imaginary part, of order $O(\beta)$, which can be obtained by setting $\tan(\gamma_\lambda/2)$ equal to $\gamma_\lambda/2$ in Eq. (45):

$$\gamma_0^2\approx-2i\beta \quad\text{and}\quad \lambda_0\approx1+i\frac{\beta}{2}.$$

All the other eigenvalues are considerably smaller, and we shall estimate them shortly.

For an arbitrary value of β, the approximate solutions γ_λ and the associated eigenvalues λ naturally separate into two classes according to whether $|\gamma_\lambda|\ll\beta$ of $|\gamma_\lambda|\gg\beta$. For large values of β, it is possible to treat the intermediate range $|\gamma_\lambda|\sim\beta$ as well; indeed, the maximum values of the real and imaginary parts of the eigenvalues occur in this range. Details may be found in Appendix B. Here we present only the final expressions.

1. Even-mode eigenvalues

(a) $|\gamma_\lambda|\ll\beta$. The mth root of Eq. (45), correct to order $O((2m+1)\pi/\beta)$, and the associated eigenvalue, correct to $O(1/\beta)^4$, are

$$\gamma_m=(2m+1)\pi-\frac{2i(2m+1)\pi}{\beta},$$

$$\lambda_m=\left[\frac{2}{\beta}+\frac{2(2m+1)^2\pi^2}{\beta^3}\right]i+\frac{8(2m+1)^2\pi^2}{\beta^4}. \quad (49)$$

Obviously, these expressions are consistent with the requirement $|\gamma_\lambda|\ll\beta$ only for m small enough that $(2m+1)\pi\ll\beta$.

(b) $|\gamma_\lambda|\gg\beta$. In this limit the mth root, correct to order $O(\beta/(2m\pi))$, and the associated eigenvalue, correct to order $O(\beta)^2$, are

$$\gamma_m=2m\pi-\frac{i\beta}{m\pi}, \quad \lambda_m=\frac{\beta^2}{2m^4\pi^4}-\frac{i\beta}{2m^2\pi^2}. \quad (50)$$

Because of the requirement $|\gamma_\lambda|\gg\beta$, only eigenvalues with m large enough that $2m\pi\gg\beta$ are well approximated by Eq. (50).

(c) $|\gamma_\lambda|\sim\beta$: *maximum Re λ and Im λ, and validity of neglect of retardation of the envelopes.* The largest real and imaginary parts of all the eigenvalues are located in this region, and approximate expressions for them can be derived for large β, although there is no simple approximate formula for all of the roots in this region. As shown in Appendix B, the maximum values of Re λ and Im λ are given by the relation

$$\max(\text{Re }\lambda)\approx2\max(\text{Im }\lambda)\approx\frac{1}{\log(2\beta/\log2\beta)}. \quad (51)$$

Based on the expression (51), we can state a quantitative criterion for the validity of the rapid-transit approximation on which our one-dimensional treatment is largely based. For the approximation to hold, it is clearly sufficient for the shortest time scales over which the field envelopes vary, i.e., the reciprocal of the largest decay rate and frequency shift (51), to be long compared to the maximum retardation interval, which is the transit time of light through the one-dimensional medium. Thus we require, in physical units, that

$$\frac{L}{c\tau_R}\ll\log\left(\frac{2\beta}{\log2\beta}\right).$$

Since the logarithmic right-hand side of this inequality is in practice never of an order of magnitude much larger than unity, the inequality is substantially equivalent to a simpler one,

$$L\ll c\tau_R,$$

which, in view of definition (20), is in turn equivalent to the inequality

$$L\ll L_c\equiv c\left(\frac{3\hbar}{n_0|\vec{\mu}|^2\omega_0}\right)^{1/2}. \quad (52)$$

The parameter L_c is essentially the cooperation length, defined by Arecchi and Courtens [17], that characterizes the maximum distance over which a medium of coherently excited atoms can cooperate and emit purely superradiant light. For typical gas densities and natural lifetimes of isolated atoms, L_c can be comfortably large, as large perhaps as thousands to hundreds of thousands of wavelengths, and thus poses no real obstacle to experimental observation of the effects predicted in the paper.

As an overall characterization of the behavior of the eigenvalues, we note that for fixed β the decay rates of the modes first rise quadratically with the mode label m according to Eq. (49), and eventually fall quartically with m^{-1} according to Eq. (50). The imaginary parts of the eigenvalues, that represent the frequency shifts of the modes from the

atomic resonance, on the other hand change sign as the associated γ_λ values cross from class (a) into class (b). The variations of the real and imaginary parts of the eigenvalues λ_m with increasing value of the mode index m bear a considerable resemblance to the linear dispersion curves for the real and imaginary parts of the susceptibility of a continuous medium with a single resonance. This analogy is discussed in further detail in Appendix B.

2. Odd-mode eigenvalues

For a fixed value of β, approximate perturbative expressions for the roots of Eq. (47) may be derived, as we show in Appendix B, much as they are for the even modes. Once again, the roots fall into two classes according to whether $|\gamma_\lambda| < \beta$ or $|\gamma_\lambda| > \beta$, but we need not say more here than that their discussion is quite parallel to that for the even-mode roots. There is one distinction, however: In the limit of a thin slab, $\beta \ll 1$, all of the odd modes correspond to trapped polarization. In the other extreme case of a thick slab, $\beta \gg 1$, all of the eigenmodes, whether even or odd, tend to become perfectly trapped.

D. Numerical evaluation of the eigenvalues

The approximate formulas that we derived for the roots of the eigenvalue equations (45) and (47) are quite accurate in the two regions $|\gamma_\lambda| \ll \beta$ and $|\gamma_\lambda| \gg \beta$, but in the intermediate region $|\gamma_\lambda| \sim \beta$ we have no recourse but to compute the roots numerically. An iterative procedure, described in Appendix B, was employed for the purpose.

In Figs. 1(a) and 1(b), we have displayed the real and imaginary parts of the eigenvalues λ for the first four of the even modes as functions of β. For each of the modes, the real part of the eigenvalue has a maximum in accordance with the general form of Eq. (B8), the mth mode having a peak at a value $\beta_m \approx 2m\pi$ for large m. Note the slow decrease of the peak values of the successive modes, which has a logarithmic character given by Eq. (51). On the other hand, the imaginary part, the scaled frequency shift of a mode, crosses from negative to positive values at about the same places as the peaks in the plot of the real part, in accordance with the structure of Eq. (B9).

A somewhat different representation of the eigenvalues is provided by Figs. 2(a) and 2(b), where we have plotted Re λ and Im λ as functions of the mode index m for four values of β. Once again, the peaked nature of the first of these plots agrees with the general relation (B8) while the zero-crossing contained in Eq. (B9) characterizes the second of these plots.

The slow logarithmic decrease of the largest of the scaled decay rates and frequency shifts of the modes, as predicted by Eq. (51), is exhibited in Figs. 3(a) and 3(b), where the plots show these largest values as a function of β for values of β as high as 10^6. Even for such large β, our iterative method worked quite rapidly to produce hundreds of thousands of roots in a matter of minutes on a Pentium Pro200 computer. These plots are semilogarithmic in order to accommodate the large range of β. We have shown our two-term asymptotic result (51) by a solid curve. Note the excellent accuracy of this result when compared with our
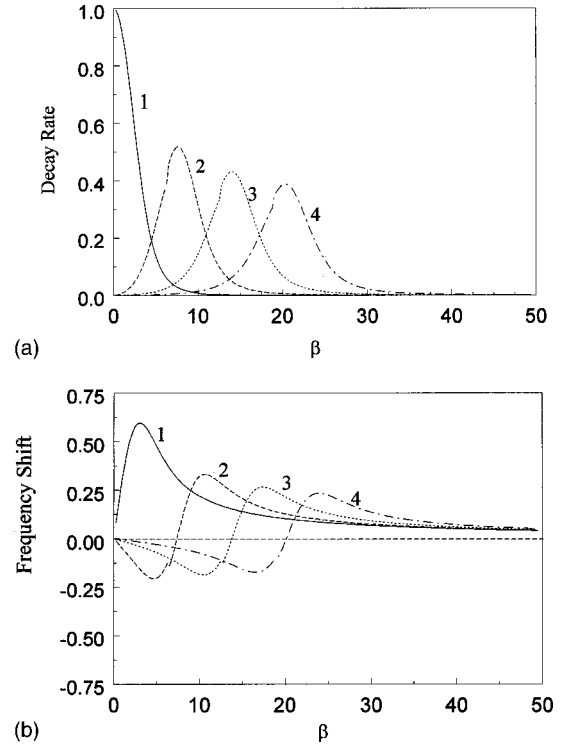

FIG. 1. (a) Decay rates Re λ_m and (b) frequency shifts Im λ_m, both in units of τ_R^{-1} as defined by Eq. (20), for the first four even modes as functions of β.

numerically obtained results, shown here by crosses, for large values of β.

VI. GENERAL TIME-DEPENDENT PROBLEM IN ONE DIMENSION

Once we have determined the eigenvalues λ characteristic of the one-dimensional problem posed by Eq. (21), we are in a position to study the temporal evolution of an arbitrary initial polarization $\mathcal{P}(Z,0)$. If this function possesses the mode expansion

$$\mathcal{P}(Z,0) = \sum_\lambda c_\lambda P_\lambda(Z), \tag{53}$$

with the expansion coefficients c_λ given by the overlap integrals

$$c_\lambda = \int_{-1/2}^{1/2} \mathcal{P}(Z,0) P_\lambda(Z) dZ, \tag{54}$$

then the time-dependent solution to Eq. (21) is

$$\mathcal{P}(Z,T) = \sum_\lambda c_\lambda P_\lambda(Z) e^{-\lambda T}. \tag{55}$$

The total energy lodged in the polarization of the medium is proportional, as we have noted in Sec. IV, to the expression
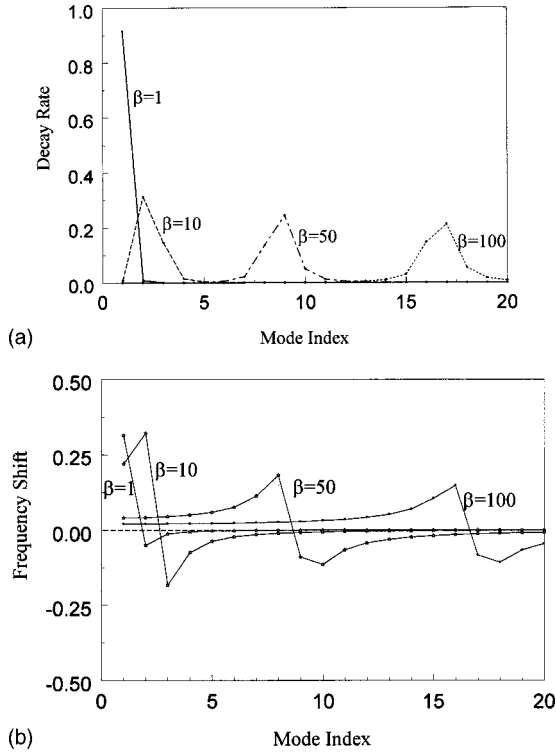
FIG. 2. (a) Decay rates Re λ_m and (b) frequency shifts Im λ_m, both in units of τ_R^{-1}, as functions of the mode index m, for $\beta=1$, 10, 50, and 100. The straight segments joining the discrete points are provided only to indicate the behavior of the eigenvalues with increasing mode index.

$$W(T)=\int_{-1/2}^{1/2}|\mathcal{P}(Z,T)|^2 dZ. \tag{56}$$

Because the orthonormality relation (27) does not involve complex conjugation, expression $W(T)$ does not, in general, reduce to a sum of contributions from the individual decaying modes. We find in addition a sum containing important cross-relaxation terms contributed by pairs of excited modes:

$$W(T)=\sum_\lambda |c_\lambda|^2 e^{-2\,\mathrm{Re}\,\lambda T}\int_{-1/2}^{1/2}dZ|P_\lambda(Z)|^2$$
$$+\sum_{\lambda\neq\lambda'} c_\lambda^* c_{\lambda'} e^{-(\lambda^*+\lambda')T}\int_{-1/2}^{1/2}dZ P_\lambda^*(Z)P_{\lambda'}(Z). \tag{57}$$

The interference terms can cause interesting behavior in the time dependence of $W(T)$, as we shall presently see, even though $W(T)$ must decrease monotonically with time T for all times, according to Eq. (22).

A. Direct numerical integration for the time evolution

Use of the mode functions and their eigenvalues to write down the general time dependence of an arbitrary excitation has given us valuable physical insight into the nature of the decay of both the amplitude of polarization and the associated energy. But the final expressions for these quantities can
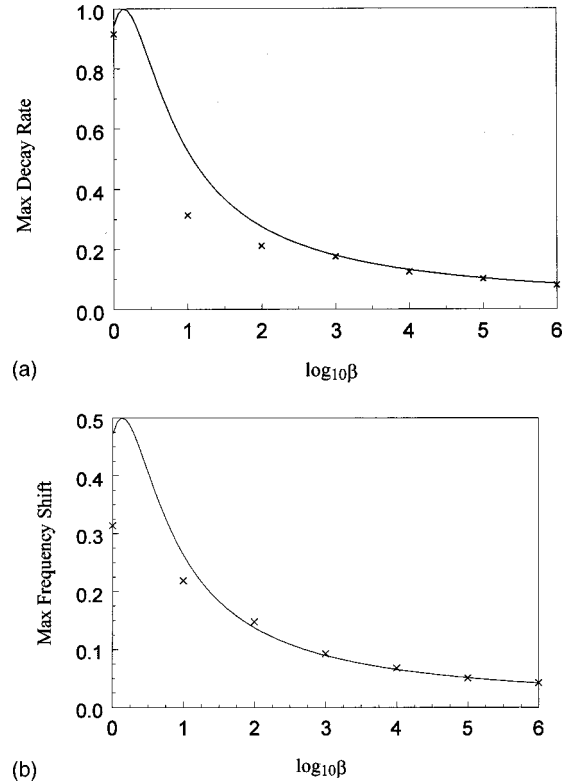

FIG. 3. (a) Maximum decay rates and (b) frequency shifts, both in units of τ_R^{-1}, as functions of β. The approximate analytical formulas (51) are shown by solid curves, while the numerically computed values are exhibited by crosses.

only be given as sums over modes, which may be awkward to evaluate. Alternatively, we can integrate the integral equation (21) directly in numerical terms. By choosing time and position steps ΔT and ΔZ that are small compared to the reciprocal of the largest decay rate (51) and β, respectively, we see from Eq. (21) that the value of $\mathcal{P}(Z,T)$ at time point T is obtained, to an excellent approximation, in terms of the values $\mathcal{P}(Z',T-\Delta T)$ at the previous time step from the relation

$$\mathcal{P}(Z,T)=P(Z,T-\Delta T)-\Delta T\Delta Z\sum_{Z'} e^{i\beta|Z-Z'|}\mathcal{P}(Z',T-\Delta T). \tag{58}$$

We have used this relation to solve for the time dependence numerically with high accuracy for two varieties of symmetric distributions of the initial polarization amplitude, the Gaussian form

$$\mathcal{P}(Z,0)=e^{-Z^2/(2\sigma^2)}, \tag{59}$$

and the step-function form

$$\mathcal{P}(Z,0)=\begin{cases} 1 & \text{for } |Z|<\sigma \\ 0 & \text{otherwise}. \end{cases} \tag{60}$$

In both cases 2σ represents the characteristic width of the initially excited region.
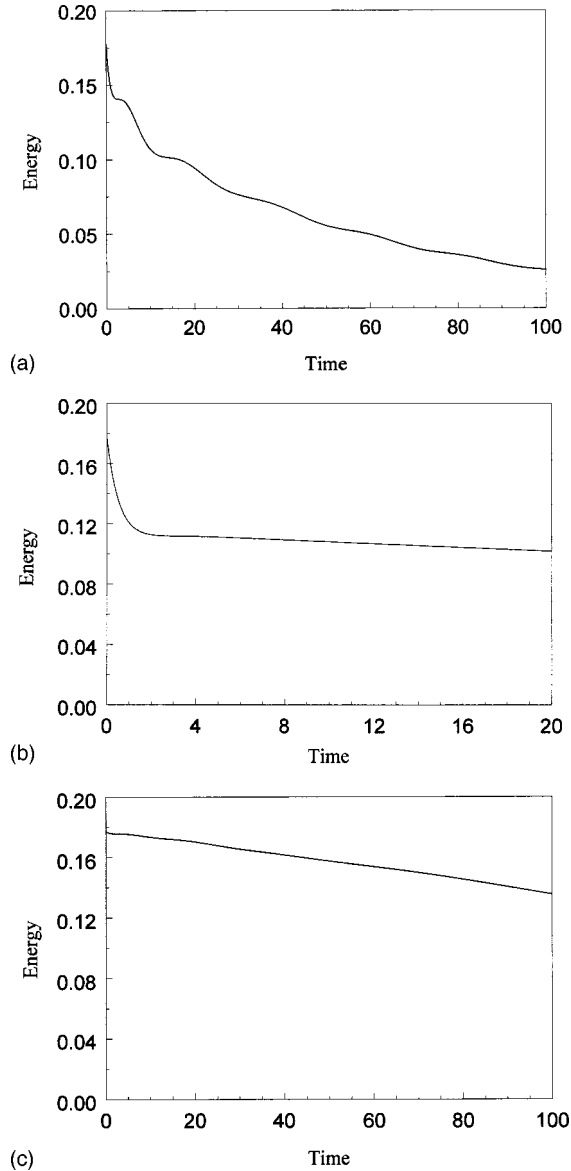
FIG. 4. The decay of the total polarization energy, in arbitrary units, as a function of time, in units of τ_R, for the initially Gaussian excitation of Eq. (59) for (a) $\beta=10$, $\sigma=0.1$; (b) $\beta=1$, $\sigma=0.1$; and (c) $\beta=20$, $\sigma=0.1$.

In Fig. 4(a), we plot the numerically obtained time dependence of the polarization energy $W(T)$ given by Eq. (56) for a polarization amplitude $P(Z,T)$ that is initially real and has a Gaussian form (59) with $\sigma=0.1$ and $\beta=10$. The plot has several features that can be understood in terms of the underlying eigenfunction decomposition (55). The initially steep, approximately exponential, drop of $W(T)$ represents the radiation of the fastest decaying eigenmode, which for $\beta=10$ has an energy decay rate $2\,\mathrm{Max}(\mathrm{Re}\,\lambda)\approx0.63$. The subsequent decay is characterized by plateaus that punctuate periods of nearly exponential damping of energy. These exponential decay stages correspond to the radiation of the progressively more slowly decaying eigenmodes, with energy decay rates $2\,\mathrm{Re}\,\lambda$ equal to 0.30, 0.03, 0.02, and smaller, that we have already presented in Fig. 2(a). The plateaus, on the

other hand, represent periods of greatly slowed radiation of the medium and arise from the interference of modes, contained in the $\lambda\neq\lambda'$ terms of Eq. (57). The interference terms in $W(T)$ evolve at rates that are determined both by the sums of the decay rates and the differences of the frequency shifts of the various mode pairs. Without such interferences, the energy $W(T)$ would have been a superposition of pure decaying exponentials with positive coefficients, and as such the slope of the energy decay curve would have decreased monotonically with time.

The interferences and the associated plateaus are most pronounced for values of β that are around 10. They are nearly absent for much smaller values of β, as for $\beta=1$ [Fig. 4(b)], since for thin samples the modes are essentially real, $P_\lambda^*(Z)\approx P_\lambda(Z)$, so that the mode overlap integrals in Eq. (57) are quite small when $\lambda\neq\lambda'$. Furthermore, only one mode, the one that is spatially uniform, has a large decay rate while the others tend not to decay at all. The decay of this fundamental mode is easily seen on the figure, while the energy in the remaining modes tends to remain trapped.

For values of β much larger than 10, the time dependence of W again loses the interesting attributes of the $\beta=10$ case. To create a Gaussian initial excitation (59) with $\sigma=0.1$, one need only excite modes for which the wave vectors γ_λ are in magnitude no larger than of order $1/\sigma=10$. But the fastest decaying modes have wave vectors γ_λ nearly equal in magnitude to β, which for $\beta\gg10$ thus tend to be absent from our initial value problem. We see in Fig. 4(c) that for $\beta=20$ there is only a small initial drop in the energy with time, because the fastest decaying modes are largely absent in the expansion (53). A close examination of the subsequent time dependence reveals low-amplitude ripples, arising from interferences, but the structure of plateaus and exponential decay periods is evidently difficult to discern.

In the next set of figures, Figs. 5(a)–5(c), we have displayed, for $\beta=10$, the spatial distribution of the real part, the imaginary part, and the squared modulus of the polarization at three different times, $T=0,5,$ and 20. By $T=5$, the fastest decaying mode with a characteristic decay period of order $1/0.63\approx1.6$ has been almost completely radiated away, while the other modes have evolved only partially. This picture suggests that by the time $T\approx1.6$, the polarization amplitude must have developed spatial oscillations. They result from a subtraction of the oscillatory amplitude distribution $c_\lambda P_\lambda(Z)$ from the smooth initial polarization amplitude. Such spatial oscillations are clearly present in all three figures. With the passage of time, more and more oscillations develop that represent the removal of successively decaying modes.

Similar features to those described above also occur in the time dependence of an initial step-function distribution of polarization. For $\beta=10$ and a uniform initial excitation with a half-width $\sigma=0.1$, the energy has a time dependence, shown in Fig. 6(a), that exhibits a somewhat slower decay than for the Gaussian initial excitation, although the qualitative features are nearly the same. This relative slowness of the overall time dependence has to do with the fact that, to create a sharply discontinuous excitation, we must superpose a substantially larger number of eigenmodes than are necessary for the smoother Gaussian profile of the same ef-
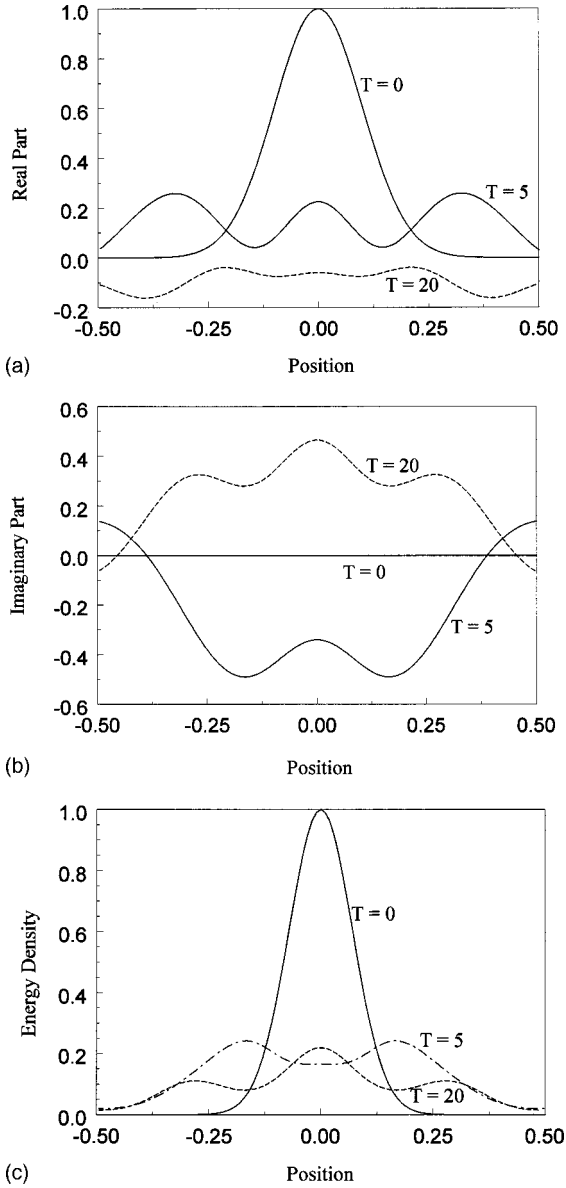
(a)

(b)

(c)

FIG. 5. The distributions of (a) the real part, (b) the imaginary part, and (c) the squared modulus of the polarization, in arbitrary units, as functions of the scaled spatial variable $Z = z/L$, for the initially Gaussian excitation of Eq. (59) at three different times, in units of τ_R, for $\beta = 10$ and $\sigma = 0.1$.

fective width. This means that a larger fraction of the energy resides, for the step-function initial excitation, in modes that have a slower decay than for the smoother Gaussian initial profile. This fact is also directly observed in Fig. 6(b), where we have plotted the real part of the polarization amplitude at different times. Note that the slow decay of the higher harmonic modes leads to a persistence of the sharp step discontinuities even at long times. The oscillations in the wings have an origin similar to those for the Gaussian case.

The oscillations are more directly seen in the time evolution of the polarization energy density at a fixed position and the power radiated by the medium. In Fig. 7(a) we display the polarization energy density at the boundaries, $Z = \pm 1/2$, for $\beta = 10$, and a symmetric step-function initial excitation of
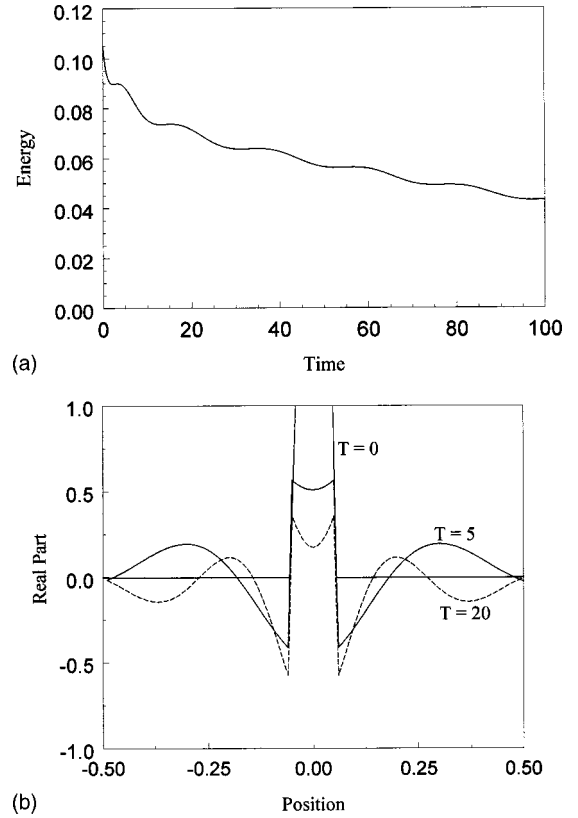

(a)

(b)

FIG. 6. (a) The decay of the total polarization energy, in arbitrary units, as a function of time, in units of τ_R, and (b) the distribution of the real part of the polarization at three different times, in units of τ_R, for an initial step-function excitation given by Eq. (60) with $\sigma = 0.05$.

half-width $\sigma = 0.2$. This energy density, proportional to $|\mathcal{P}(Z = \pm 1/2, T)|^2$, is initially zero, but builds up quite rapidly in an oscillatory fashion and eventually decays away at long times. The ringing oscillations, which are similar to those of Burnham and Chiao [10] but somewhat less regular, arise from a coherent exchange of energy between different regions of the medium by means of the electromagnetic field. The radiated power undergoes a similar ringing. The plot of $|\partial \mathcal{P}(Z = \pm 1/2, T)/\partial T|^2$, which, by Eq. (14), is proportional to the radiated power, is shown versus the time T in Fig. 7(b). The initial sharp spike, not entirely contained in the figure because of its large amplitude, arises from the radiation of the fastest decaying mode. The oscillations in the two figures, Figs. 7(a) and 7(b), have commensurate patterns, with the maxima of one coinciding with the minima of the other.

B. Frequency spectrum of radiated power

The presence of vastly differing decay rates and frequency shifts of the eigenmodes leads to the possibility of interesting spectral distributions of radiation. Because each eigenmode undergoes exponential decay, the power spectrum it radiates has a simple Lorentzian shape. Its characteristic half-width and frequency shift from the atomic resonance are, respectively, equal to the real and imaginary parts of the associated eigenvalue. An arbitrary initial polarization
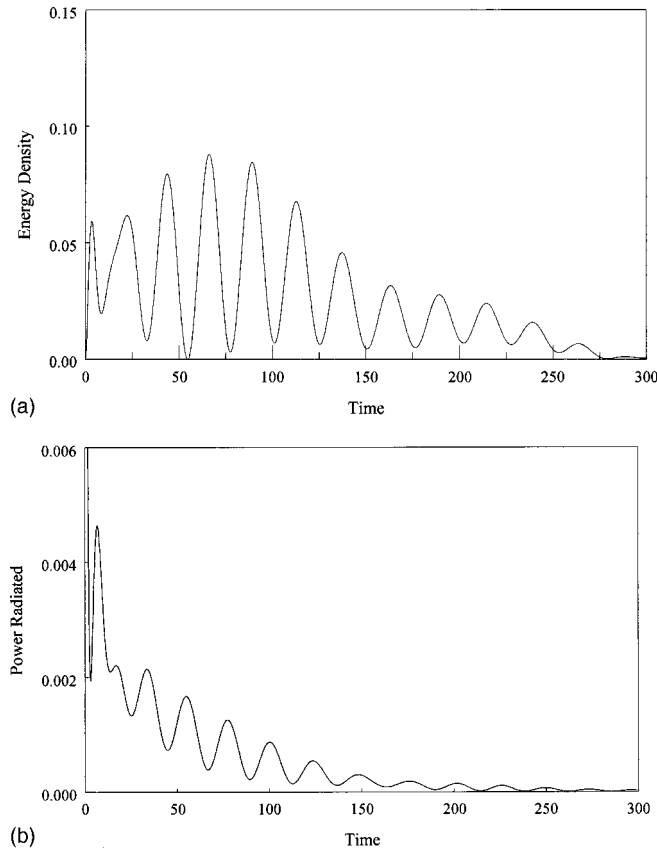
FIG. 7. (a) The polarization energy density at the boundaries and (b) the power radiated by the medium, both in arbitrary units, as functions of time, in units of τ_R, for an initial excitation given by Eq. (60) with $\beta = 10$ and $\sigma = 0.2$.

distribution, regarded as a coherent superposition of eigenmodes, will emit radiation with a power spectrum that consists of a sequence of Lorentzian peaks for the individual modes as well as cross-spectral interferences that can change the shape of the spectrum significantly and lead to sharply resonant dips. Resonant dips of this and less symmetric sorts are familiar in the energy dependence of nuclear cross sections, which often contain interferences between competing resonances. They are somewhat more novel in the context of atomic spectra, where they are called Fano resonances [19].

Because of the separation of the time scales of successively decaying modes, as in Fig. 4(a), for example, there is an interesting sense in which the spectra observed over appropriately short time intervals can be regarded as varying with time. Here, however, we shall only derive the more customary spectra associated with long measurement times.

For a time-dependent polarization of form (55), the spectral amplitude at a scaled frequency detuning ν is proportional to the Fourier transform,

$$Q(Z,\nu) = \int_0^\infty \mathcal{P}(Z,T)e^{i\nu T}dT = \sum_\lambda \frac{c_\lambda}{\lambda - i\nu} P_\lambda(Z). \quad (61)$$

The spectrum of the radiated intensity is in turn proportional to the squared modulus, $S(Z,\nu) = |Q(Z,\nu)|^2$, evaluated at the boundaries $Z = \pm 1/2$.

Our numerical treatment of the radiated spectra begins with an evaluation of the complex amplitudes c_λ of Eq. (54) for a variety of initial polarization distributions $\mathcal{P}(Z,0)$. We then use these amplitudes and the numerically evaluated eigenvalues λ in Eq. (61) to find the spectra. This approach proves to be considerably simpler than taking the Fourier transform of the numerically calculated time dependence of the polarization.

In Figs. 8(a)–8(c), we show the spectra of power radiated by step-function initial polarization distributions in media of three different values of β, 1, 10, and 50. A symmetric excitation of the medium, as in all but the bottom part of Fig. 8(b), contains only the even eigenmodes, and therefore radiates a spectrum with a resonant structure provided only by those modes. When the excitation is localized at a boundary of the medium, the spatial symmetry is broken and the radiated spectrum consists of peaks arising from the odd modes as well, as can be seen clearly in the bottom half of Fig. 8(b). The even and odd modes are interleaved in their frequency shifts, as noted earlier, and that leads to a doubling of the number of peaks in the spectrum when compared with the upper half of Fig. 8(b). In the bottom half of Fig. 8(a), corresponding to a symmetric excitation that uniformly spans 98% of the medium initially, the dominant excitation is that of the nearly uniform superradiant mode. Its spectrum provides the broad background in the figure. The small admixture of other, more slowly decaying modes, however, leads to sharp resonant dips as well as peaks impressed upon the broad spectrum. The dips, in particular, are due to the destructive cross-spectral interferences between the dominant superradiant mode and the weaker, more slowly decaying modes.

There is also a frequency gap for the larger values, 10 and 50, of β, in which no significant radiation is present. All of the central frequencies of the radiating modes tend to accumulate near the two boundaries of the gap. Unmistakable in Fig. 8(c) and in the top curve in Fig. 8(b), it represents, as suggested by the approximate expressions (B4) and (B7), the absence of eigenmodes with a frequency shift in the interval from 0 to $2/\beta$ for $\beta \gg 1$. The gap arises from the inability of waves of frequencies in that interval to propagate freely inside the medium. For frequencies within that interval, the corresponding γ_λ, according to Eq. (48), would have to be essentially purely imaginary and the modes would be exponentially damped according to Eqs. (44) and (46). An initial excitation close to the surface of the medium, on the other hand, can still emit at frequencies lying within the gap, as shown by Fig. 8(b), since the radiation does not have to travel any significant distance within the medium. The light radiated from the surface opposite to the excitation, by contrast, has to traverse nearly the entire medium, and must therefore show this frequency gap clearly.

That the frequency gap must all but disappear for thin samples with $\beta = k_0 L < 1$ is also evident from the same argument. To see this, we first note that since for any eigenvalue λ its imaginary part representing the frequency shift dominates its real part, which represents its decay rate, we may write Eq. (48) approximately as

Spectrum of Radiated Power

(a)

Spectrum of Radiated Power
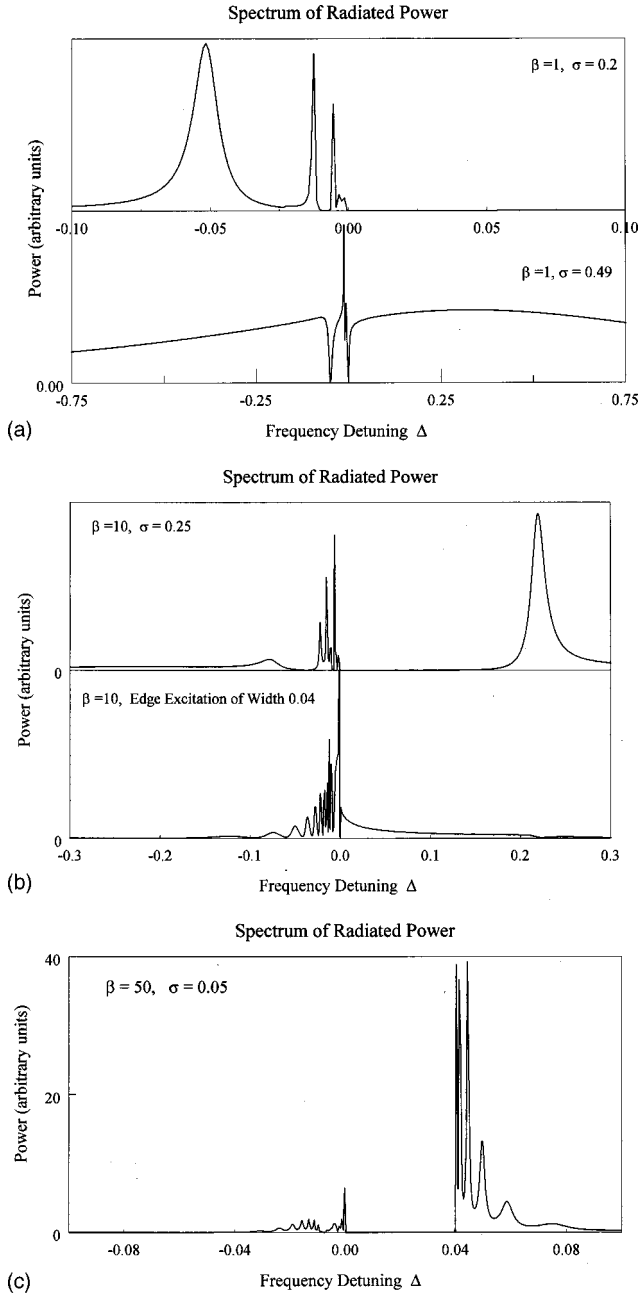
(b)

Spectrum of Radiated Power

(c)

FIG. 8. The frequency spectrum of the power radiated by the medium, in arbitrary units, with (a) $\beta=1$ and $\sigma=0.2$ (upper figure); $\beta=1$, $\sigma=0.49$ (lower figure); (b) $\beta=10$ and $\sigma=0.2$ (upper figure); initial excitation confined to the region between $Z=0.46$ and 0.50 with $\beta=10$ (lower figure); and (c) $\beta=50$ and $\sigma=0.05$. The abscissa represents frequency detuning in units of τ_R^{-1}. The parameter σ is the fractional half-width of the region, which has a uniform initial excitation and sharply defined boundaries.

$$\text{Im}\,\lambda = \frac{2\beta}{\beta^2 - \gamma_\lambda^2}.$$

On inverting this relation to express γ_λ as a function of $\text{Im}\,\lambda$, we can see that only in the range of frequency shifts $0 < \text{Im}\,\lambda < 2\beta/(1+\beta^2)$, which vanishes as $\beta \to 0$, is γ_λ appreciably imaginary, exceeding 1 in magnitude. Consequently,

only in this range of frequency shifts is there a significant exponential attenuation of the fields, as they propagate through the medium.

Within the gap, the interference and resonant interaction between the forward- and backward-traveling waves is too strong for the light to be able to leave the medium. By contrast, for the Burnham-Chiao problem [10] the spectrum of the radiated field, which is readily evaluated, contains no frequency gap because it neglects the backward waves completely. It does show, however, an accumulation of ever faster oscillations in the spectrum as the resonance frequency, renormalized by the field-medium interaction, is approached from either side. These accumulations of peaks are evidently analogous to the accumulations of mode frequencies seen in Figs. 8(b) and 8(c) at the two edges of the frequency gap in our problem.

C. Decay of a sharply localized symmetric excitation

A problem of some interest concerns the time dependence of the polarization and the total excitation energy when the slab has initially a sharply localized excitation, which we shall take to be of the Gaussian form (59). We shall assume further that the width, σL in physical units, of the initially excited region is small compared to the wavelength. We assume, in other words, that $\sigma \ll \min(1,1/\beta)$.

For this problem, the expansion coefficients in the solution (55) take the form

$$c_n = \int_{-1/2}^{1/2} e^{-Z^2/(2\sigma^2)} P_n(Z)dZ,$$

which can be evaluated by noting that, for $\sigma \ll 1$, the limits of integration may be extended to $\pm\infty$ without significant loss of accuracy. Since the symmetric eigenfunctions (44) are just cosines, the preceding integral can then be evaluated in a closed form:

$$c_n \approx \sqrt{\frac{4\pi\sigma^2}{1+\sin\gamma_n/\gamma_n}} e^{-\gamma_n^2\sigma^2/2}. \tag{62}$$

Note that, since $\gamma_n \approx 2n\pi$ for large n, a number, roughly of order $1/(2\pi\sigma)$, of the c_n have a significant amplitude. For σ sufficiently small compared to $1/(2\pi)$, this number can be large. Furthermore, since $\sigma \ll 1/\beta$, this number also greatly exceeds $\beta/(2\pi)$. Under such conditions, a large part of the excitation may reside in modes for which $|\gamma_n| \gg \beta$, and which decay rather sluggishly according to the result (50). It is, then, precisely these modes that would govern the long-time behavior of the decaying polarization. These modes have amplitudes [Eq. (62)] in which the γ_n may be replaced by their approximate values $2n\pi$. Ignoring small terms of order $1/(2n\pi)$, we have finally the result

$$c_n \approx \sqrt{4\pi\sigma^2}\, e^{-2n^2\pi^2\sigma^2}. \tag{63}$$

By using in Eq. (55), the eigenvalues (50), eigenfunctions (44), and coefficients (63) as well as our approximation, $\gamma_n \approx 2n\pi$, we may express the long-time behavior of $\mathcal{P}(Z,T)$ accurately as

$$\mathcal{P}(Z,T) \approx \sqrt{8\pi\sigma^2} \sum_n e^{-2n^2\pi^2\sigma^2} \cos(2n\pi Z)$$

$$\times \exp\left[-\left(\frac{\beta^2}{2n^4\pi^4} - \frac{i\beta}{2n^2\pi^2}\right)T\right]^{1/2}. \quad (64)$$

Since, for $2n\pi \gg \beta$,

$$\mathrm{Re}\,\lambda_n \approx \frac{\beta^2}{2n^4\pi^4} \ll \mathrm{Im}\,\lambda_n \approx \frac{\beta}{2n^2\pi^2},$$

it seems plausible that the evolution of the polarization amplitude is dictated more by the dephasing of the oscillations of the successive modes, because of their different frequency shifts, than by the decaying mode amplitudes. We shall assume this to be true for the moment, and then verify that it is an acceptable approximation. Ignoring the decay rates for the temporal evolution of the polarization amplitude $\mathcal{P}(Z,T)$, we have

$$\mathcal{P}(Z,T) \approx \sqrt{8\pi\sigma^2} \sum_n e^{-2n^2\pi^2\sigma^2} \cos(2n\pi Z) e^{(i\beta/2n^2\pi^2)T}. \quad (65)$$

By contrast, it follows from Eq. (64), and the orthogonality relation

$$\int_{-1/2}^{1/2} \cos(2n\pi Z)\cos(2m\pi Z)dZ = \tfrac{1}{2}\delta_{mn}, \quad m,n>1,$$

that the polarization energy (56) has the long-time behavior

$$W(T) \approx 4\pi\sigma^2 \sum_n e^{-4n^2\pi^2\sigma^2} e^{-(\beta^2/n^4\pi^4)T}, \quad (66)$$

which is thus affected only by the decay rates of the modes. Furthermore, Eq. (66) contains no mode-mode interference terms, which tend to be present only over relatively short times.

As a special case, we consider the long-time evolution of the polarization amplitude at the midpoint $Z=0$ in the slab, for which all of the cosines in Eq. (65) are unity. Since the term inside the sum there changes very little as n is changed by one unit, particularly when n is large, we may replace the sum by an integral over n with limits 0 and ∞, and thereby obtain the following asymptotically correct expression:

$$\mathcal{P}(0,T) \approx \sqrt{\frac{4}{\pi}} \int_0^\infty e^{-x^2 + i\beta\sigma^2 T/x^2} dx.$$

The integral on the right can be expressed [20] in the closed form

$$\mathcal{P}(0,T) \approx e^{-\sigma\sqrt{\beta T/2}(1-i)}. \quad (67)$$

Thus even though each of the constituent modes of our initially sharply localized coherent excitation decays exponentially, the summation over a large number of such modes gives rise to a "slowed-down" subexponential decay of the superposition $\mathcal{P}(0,T)$ with a characteristic decay time

$$T_\sigma = \frac{1}{\beta\sigma^2}.$$

In physical units, this decay time has the value

$$\tau_\sigma = \frac{1}{\beta\sigma^2}\,\tau_R = \frac{6\hbar}{n_0^2|\vec{\mu}|^2\beta^2\sigma^2}, \quad (68)$$

which is inversely proportional to the square of the initial width $\sigma L = \sigma\beta/k_0$ of the excited region. The more localized the initial excitation, the longer its amplitude takes to decay via the coherent dephasing process we have mentioned earlier.

Similar results may be obtained for the decay of the total energy $W(T)$. However, because of a different dependence of the mode decay rates on the mode label n, the final result for W is qualitatively different:

$$W(T) \approx 2\sigma \int_0^\infty e^{-x^2 - 16\beta^2\sigma^4 T/x^4} dx. \quad (69)$$

The integral cannot be expressed exactly in a closed form, but it does represent a monotonically decaying function of the variable $\beta^2\sigma^4 T$. As such, its characteristic decay time must be of order

$$T_\sigma' = \frac{1}{\beta^2\sigma^4}, \quad (70)$$

or, in physical units, of order

$$\tau_\sigma' = \frac{1}{\beta^2\sigma^4}\,\tau_R = \frac{6\hbar}{n_0^2|\vec{\mu}|^2\beta^3\sigma^4}. \quad (71)$$

Since $\sigma L = \sigma\beta/k_0$ is the physical width of the initially excited region, the decay of the total energy extends over a time that increases linearly with the slab thickness L and quartically with $1/\sigma$ as the initial excitation width σ becomes smaller. We also note that since we have assumed $\sigma, \beta\sigma \ll 1$, $T_\sigma' = T_\sigma^2 \gg T_\sigma$, so that the decay of the polarization amplitude takes a much shorter time than that of the total energy. This also justifies the neglect of the decay of mode amplitudes when compared to the effect of mode dephasing as the principal mechanism for the decay of polarization amplitude, proving an assertion made earlier.

The asymptotic form of the decay of W may be derived by a version of the steepest-descent method. The details of the derivation are provided in Appendix C. The long-time behavior of $W(T)$ turns out to have the form

$$W(T) \approx \sqrt{2\pi/3}\,\sigma e^{-3(4T/T_\sigma')^{1/3}},$$

which is a "stretched" exponential with a qualitatively different character and time scale from the decay [Eq. (66)] of the polarization amplitude.

VII. INCLUSION OF A NONRESONANT BACKGROUND REFRACTIVE INDEX

We have, in the interest of simplicity, to this point considered a medium we have called polarium, consisting of atoms that only interact with the field through a single resonant transition. Whatever atoms are present in an actual medium, of course, will have many spectral resonances which, though scarcely excited, contribute a certain smoothly varying background to the dramatically varying polarizability in the neighborhood of the resonant frequency ω_0. A more realistic picture of the behavior of the medium near its resonant frequency, in other words, should include a certain frequency-insensitive background refractive index σ.

The polarization density $\vec{\Pi}^{(+)}(\vec{r},t)$ contributed by other distant resonances, we may assume, follows the field $\vec{E}^{(+)}(\vec{r},t)$, essentially instantaneously with a susceptibility (σ^2-1):

$$\vec{\Pi}^{(+)}(\vec{r},t)=(\sigma^2-1)\vec{E}^{(+)}(\vec{r},t). \tag{72}$$

The quantity $\vec{\Pi}^{(+)}$ must be added to the polarization density $\vec{P}^{(+)}$ resulting from the resonant transition in Eq. (10), which generalizes that equation to

$$\left(\nabla^2-\frac{1}{c^2}\frac{\partial^2}{\partial t^2}\right)\vec{E}^{(+)}(\vec{r},t)$$

$$=\frac{1}{c^2}\frac{\partial^2}{\partial t^2}[\vec{P}^{(+)}(\vec{r},t)+(\sigma^2-1)\vec{E}^{(+)}(\vec{r},t)]. \tag{73}$$

At this point we could combine the $\vec{E}^{(+)}$ terms in Eq. (73), and seem thereby to simplify its structure. But the Green's function for the wave equation would then have to be changed to account for multiple internal reflections within the medium. It is much more convenient instead to retain the formulation of the integral equation we have already used by leaving the $(\sigma^2-1)\vec{E}^{(+)}$ term on the right-hand side of Eq. (73) intact, and treating it as an additional source term for the wave equation in free space. As a result, Eqs. (11), (13), and (15)–(17) are only modified by adding the term given by Eq. (72) to the corresponding integrands. The modified version of Eq. (17), in particular, has the form

$$\frac{\partial}{\partial t}\mathcal{P}(z,t)=-\frac{|\vec{\mu}|^2 n_0 k_0}{6\hbar}\int_{-L/2}^{L/2}[\mathcal{P}(z',t)+(\sigma^2-1)\mathcal{E}(z',t)]$$

$$\times e^{ik_0|z-z'|}dz', \tag{74}$$

while the response of the resonant polarization density $\mathcal{P}$ to the field $\mathcal{E}$ described by Eq. (15) is formally unchanged:

$$\frac{\partial}{\partial t}\mathcal{P}(z,t)=i\frac{n_0|\vec{\mu}|^2}{3\hbar}\mathcal{E}(z,t). \tag{75}$$

Eliminating $\mathcal{E}$ between Eqs. (74) and (75) yields the desired integral equation for $\mathcal{P}$, which in the scaled units defined by Eqs. (20) and (21) becomes

$$\frac{\partial}{\partial T}\mathcal{P}(Z,T)=-\int_{-1/2}^{1/2}dZ'\,e^{i\beta|Z-Z'|}$$

$$\times\left[\mathcal{P}(Z',T)-i\frac{(\sigma^2-1)\beta}{2}\frac{\partial\mathcal{P}(Z',T)}{\partial T}\right],$$

$$|Z|\leqslant 1/2. \tag{76}$$

It is worth emphasizing that $\mathcal{P}(Z,T)$ represents only a part of the total polarization density, the part that is resonant and of primary interest in this paper.

The presence of the derivative term inside the integral in Eq. (76) does not hinder formulation of Eq. (76) as an eigenvalue problem. Solutions of Eq. (76) of the form $e^{-\Lambda T}P_\Lambda(Z)$ are seen to obey the eigenvalue integral equation

$$\lambda P_\Lambda(Z)=\int_{-1/2}^{1/2}dZ'\,e^{i\beta|Z-Z'|}P_\Lambda(Z'), \tag{77}$$

in which eigenvalue λ is defined by the relation

$$\frac{1}{\lambda}=\frac{1}{\Lambda}+i\frac{(\sigma^2-1)\beta}{2}. \tag{78}$$

The integral equation (77) is identical to Eq. (21), the integral equation for the interaction with a single resonance. All of the eigenvalues and eigenfunctions are therefore the same as those that we have already discussed in the previous sections. The only change is that the eigenvalue λ and the complex decay constant Λ are no longer one and the same.

To see how the relation (78) between the decay constants and the eigenvalues affects our important conclusions, we first note that their real and imaginary parts are simply related. For σ^2 real, we have, e.g.,

$$\frac{\text{Re}\,\Lambda}{|\Lambda|^2}=\frac{\text{Re}\,\lambda}{|\lambda|^2},\quad\frac{\text{Im}\,\Lambda}{|\Lambda|^2}=\frac{\text{Im}\,\lambda}{|\lambda|^2}+\frac{(\sigma^2-1)\beta}{2}. \tag{79}$$

An immediate consequence of the first of these relations is that, like λ, all of the modified decay constants Λ also have non-negative real parts, representing a radiative damping of energy from the medium in the absence of an external energy source. This is consistent with the outgoing-wave boundary conditions (24) that are also implicit in Eq. (77).

Since the imaginary part of an eigenvalue λ_m generally dominates its real part according to the approximate expressions (B4) and (B7), it follows from Eq. (79) that

$$\frac{\text{Re}\,\Lambda}{|\Lambda|^2}\approx\frac{\text{Re}\,\lambda}{(\text{Im}\,\lambda)^2},\quad\frac{\text{Im}\,\Lambda}{|\Lambda|^2}\approx\frac{1}{\text{Im}\,\lambda}+\frac{(\sigma^2-1)\beta}{2}. \tag{80}$$

When expressions (B4) and (B7) are employed in Eq. (80), it is readily seen that the imaginary parts of the constants Λ also tend to dominate their real parts. We may thus replace $|\Lambda|^2$ in the denominators in Eq. (80) approximately by $(\text{Im}\,\Lambda)^2$. This yields the following approximate expressions for $\text{Re}\,\Lambda$ and $\text{Im}\,\Lambda$:

$$\text{Re} \,\Lambda = \frac{\text{Re} \,\lambda}{(\text{Im} \,\lambda)^2} \times (\text{Im} \,\Lambda)^2, \quad \text{Im} \,\Lambda = \frac{\text{Im} \,\lambda}{1 + \dfrac{(\sigma^2 - 1)\beta}{2} \text{Im} \,\lambda}.$$

$$(81)$$

The eigenvalues λ for the nearly trapped modes for which $\text{Re} \,\lambda$ are small, as we have seen, fall into two classes: those with $|\gamma_\lambda| \ll \beta$, and therefore positive line shifts $\text{Im} \,\lambda$; and those with $|\gamma_\lambda| \gg \beta$, and therefore negative line shifts $\text{Im} \,\lambda$. For the eigenvalues that obey the former inequality and are given by expressions (B4), formulas (81) then yield the approximate values

$$\text{Im} \,\Lambda = \frac{\text{Im} \,\lambda}{\sigma^2}, \quad \text{Re} \,\Lambda = \frac{\text{Re} \,\lambda}{\sigma^4}. \qquad (82)$$

For the eigenvalues defined by the latter inequality $|\gamma_\lambda| \gg \beta$, on the other hand, for which expressions (B7) hold, there is hardly any change in the decay rates and line shifts.

Adding a frequency-independent background susceptibility also affects the local-field corrections. On average, the local field consists of the smoothed macroscopic field $\vec{E}^{(+)}(\vec{r},t)$ plus contributions [15] of the form $\vec{P}^{(+)}(\vec{r},t)/3$ and $\vec{\Pi}^{(+)}(\vec{r},t)/3$ from the resonant and nonresonant parts of the total polarization density. The effect of the resonant part $\vec{P}^{(+)}/3$ of the local-field correction is merely to shift the resonant frequency downward, as we noted in Sec. II. We see from Eq. (72), on the other hand, that the nonresonant part $\vec{\Pi}^{(+)}/3$ adds to the macroscopic field $\vec{E}^{(+)}$ a term $(\sigma^2 - 1)\vec{E}^{(+)}/3$, which just renormalizes the resonant susceptibility by the factor $1 + (\sigma^2 - 1)/3 = (\sigma^2 + 2)/3$.

VIII. CONCLUDING REMARKS

We have developed a theory of transport of coherent excitations of a resonant medium by means of electromagnetic radiation. When incoherent processes like Doppler or collisional broadening and density fluctuations are entirely ignored, spatially extended excitations tend in general to remain trapped within the medium. The electromagnetic field can stimulate the dipoles of the medium to radiate efficiently only if the spatial distribution of their phases is similar to the spatial variation of the phase of the radiated field. Such efficiently radiating modes of excitation have an essentially superradiant character, with a characteristic rate of order τ_R^{-1} given by Eq. (36). The need for phase matching requires that these modes have wave vectors that are close in magnitude to the resonant value ω_0/c. All other polarization distributions are only weakly coupled to the radiation field. Such distributions must decay relatively slowly, if at all. They represent modes of coherent excitation of the medium that tend to remain trapped in the absence of incoherent relaxation processes.

A somewhat different physical problem that can also be described by our general theoretical model is that of reflection and transmission of a wave externally incident on an otherwise unexcited slab. That arrangement provides a different, but experimentally more accessible, way of studying the coherent resonances that we have described in the present paper.

APPENDIX A: CERTAIN SUM RULES FOR THE EIGENVALUES

From the expansion of the kernel function $\exp[i\beta|Z - Z'|]$,

$$e^{i\beta|Z - Z'|} = \sum_\lambda \lambda P_\lambda(Z) P_\lambda(Z'), \qquad (A1)$$

we can derive a succession of sum rules for the sums of integer powers of the eigenvalues. A simple example is the linear sum rule (29). To find these, we construct an nth-order product of kernel functions that takes the cyclic form

$$e^{i\beta|Z_1 - Z_2|} e^{i\beta|Z_2 - Z_3|} \cdots e^{i\beta|Z_n - Z_1|},$$

and integrate the product over the variables Z_i, $i = 1, \ldots, n$, between the limits $1/2$ and $-1/2$. When each kernel factor in the integrand is expressed by a sum of form (A1) and the orthonormality relation (27) is employed, we find a remarkably simple result. The multiple sums collapse into a single sum over the nth powers of the eigenvalues, and we obtain

$$\int_{-1/2}^{1/2} dZ_1 \int_{-1/2}^{1/2} dZ_2 \cdots \int_{-1/2}^{1/2} dZ_n \exp[i\beta(|Z_1 - Z_2|$$
$$+ |Z_2 - Z_3| + \cdots + |Z_n - Z_1|)] = \sum_\lambda \lambda^n. \qquad (A2)$$

Partial sums over all of the even-mode eigenvalues or over all of the odd-mode eigenvalues and of their powers may also be obtained quite simply from Eq. (A1). By replacing Z' by $-Z'$ in Eq. (A1), we obtain a closely related sum which, when added to and subtracted from Eq. (A1), produces two different sums: the first over all of the even modes, and the second over all of the odd modes. This is because paired sums and differences of form $P_\lambda(Z') \pm P_\lambda(-Z')$ vanish, respectively, for odd and even modes P_λ. In these even- and odd-mode sums, when Z is set equal to Z' and an integration is performed over the range $(-1/2, 1/2)$, the partial sums are found to be

$$\sum_{\lambda^{(e)}} \lambda^{(e)} = \frac{1}{2} + \frac{(e^{2i\beta} - 1)}{2i\beta}, \quad \sum_{\lambda^{(o)}} \lambda^{(o)} = \frac{1}{2} - \frac{(e^{2i\beta} - 1)}{2i\beta},$$

$$(A3)$$

where the superscripts e and o denote even and odd modes, respectively. Note the special case of a thin slab, $\beta \to 0$, for which the sum over the even-mode eigenvalues tends to 1, while that over the odd-mode eigenvalues vanishes. By following the same strategy as for the unrestricted sum (A1), we can easily derive partial sums of any power of the eigenvalues for the cases of even and odd modes.

APPENDIX B: ANALYTICAL AND NUMERICAL CONSIDERATIONS OF THE EIGENVALUES

Here we derive approximate analytical expressions for the roots of the transcendental equations (45) and (47). When either $|\gamma_\lambda| \ll \beta$ or $|\gamma_\lambda| \gg \beta$, the roots may be approximated well by simple expressions.

1. $|\gamma_\lambda| \ll \beta$

Forms for the two equations (45) and (47) that suggest simple approximations for the roots, when they obey the condition $|\gamma_\lambda| \ll \beta$, are

$$\cot(\gamma_\lambda/2) = i\gamma_\lambda/\beta \quad \text{and} \quad \tan(\gamma_\lambda/2) = -i\gamma_\lambda/\beta. \quad (B1)$$

It is obvious that the roots γ_λ for the two equations must be close to $(2m+1)\pi$ and $2m\pi$, respectively, where m is an integer. We shall henceforth label the roots γ_λ by the integer m, and suppress the subscript λ altogether. The small corrections, say ϵ_m, to these zeroth-order approximations may be obtained by requiring that the corrected expressions for the roots; that is,

$$\gamma_m = (2m+1)\pi + \epsilon_m \quad \text{and} \quad \gamma_m = 2m\pi + \epsilon_m, \quad (B2)$$

separately obey the two equations (B1). When this is done, $\tan \epsilon_m$ is set equal to ϵ_m, and ϵ_m is ignored in the ratio γ_m/β—a procedure that is clearly valid for small ϵ_m—the results are the following two-term expressions for the roots for the two equations (B1):

$$\gamma_m = (2m+1)\pi - i\frac{2(2m+1)\pi}{\beta}$$

$$\text{and} \quad \gamma_m = 2m\pi - i\frac{4m\pi}{\beta}. \quad (B3)$$

The eigenvalues now follow from Eq. (48), and to order $O(1/\beta)^4$, are

$$\lambda_m = \left[\frac{2}{\beta} + \frac{2(2m+1)^2\pi^2}{\beta^3}\right]i + \frac{8(2m+1)^2\pi^2}{\beta^4}$$

$$\text{and} \quad \lambda_m = \left(\frac{2}{\beta} + \frac{8m^2\pi^2}{\beta^3}\right)i + \frac{32m^2\pi^2}{\beta^4}, \quad (B4)$$

respectively. Note that roots (B3) for the even and odd modes are interleaved along the line joining the origin and the point $(1-2i/\beta)$ in the complex γ_λ plane. As a final comment, we note that consistency with the requirement $|\gamma_\lambda| \ll \beta$ implies that for the two cases only those eigenvalues for which $(2m+1)\pi \ll \beta$ and $2m\pi \ll \beta$ are well approximated by expressions (B4).

2. $|\gamma_\lambda| \gg \beta$

For this situation, we write the two transcendental equations in a form that exhibits the ratio β/γ_λ on their right-hand sides:

$$\tan(\gamma_\lambda/2) = -i\beta/\gamma_\lambda \quad \text{and} \quad \cot(\gamma_\lambda/2) = i\beta/\gamma_\lambda. \quad (B5)$$

As for situation (a), we may label the roots again by an integer index m, and by means of a perturbative procedure very similar to that used above, we can easily show that the roots take on the values

$$\gamma_m = 2m\pi - i\frac{\beta}{m\pi} \quad \text{and} \quad \gamma_m = (2m+1)\pi - i\frac{2\beta}{(2m+1)\pi}, \quad (B6)$$

for the even and odd modes, respectively. The eigenvalues now follow from Eq. (48), and to order $O(\beta)^2$ are

$$\lambda_m = \frac{\beta^2}{2m^4\pi^4} - i\frac{\beta}{2m^2\pi^2}$$

$$\text{and} \quad \lambda_m = \frac{8\beta^2}{(2m+1)^4\pi^4} - i\frac{2\beta}{(2m+1)^2\pi^2}. \quad (B7)$$

Because of the requirement $|\gamma_\lambda| \gg \beta$, only eigenvalues with $2m\pi \gg \beta$ and $(2m+1)\pi \gg \beta$ are well approximated by the two expressions of Eq. (B7). For large m, the eigenvalues for the even and odd modes are again close to each other.

3. Distribution of real and imaginary parts of eigenvalues and the intermediate regime $|\gamma_\lambda| \sim \beta \gg 1$

This intermediate case is much harder to treat and, in fact, no general analytical approximations of high accuracy have been found. It is possible, however, to find accurate approximations for the maxima in the real and imaginary parts of the eigenvalues when they are plotted as functions of β for large values of β. To do so, we need to understand better the distributions of the real and imaginary parts.

From Eq. (48), the real and imaginary parts of the eigenvalues λ_m may be expressed in terms of the real and imaginary parts of γ_m^2 as

$$\text{Re}\,\lambda = \frac{-2\beta\,\text{Im}\,\gamma_\lambda^2}{[\beta^2 - \text{Re}\,\gamma_\lambda^2]^2 + [\text{Im}\,\gamma_\lambda^2]^2}, \quad (B8)$$

$$\text{Im}\,\lambda = \frac{2\beta[\beta^2 - \text{Re}\,\gamma_\lambda^2]}{[\beta^2 - \text{Re}\,\gamma_\lambda^2]^2 + [\text{Im}\,\gamma_\lambda^2]^2}. \quad (B9)$$

As Eqs. (B3) and (B6) suggest, γ_m^2 has only a small imaginary part, while its real part increases essentially quadratically with the mode index m. As a result, for fixed β, the distribution (B8) of the real parts of the eigenvalues λ_m is highly peaked, as a function of m, around $m \approx \beta/(2\pi)$, while the distribution (B9) of the imaginary parts of the eigenvalues changes sign. This behavior is quite analogous to that of the real and imaginary parts of the complex susceptibility of a dielectric medium with a single resonance frequency when the frequency of incident monochromatic radiation is tuned through the resonance.

We shall now exploit this structure to compute the maximum values of $\text{Re}\,\lambda$ and $\text{Im}\,\lambda$ as functions of β. According to Eq. (B8), the largest value of $\text{Re}\,\lambda_m$ is obtained roughly when β has a value for which one of the allowed values of γ_m^2 obeys the equality

$$\beta = \sqrt{\text{Re } \gamma_m^2} = \sqrt{(\text{Re } \gamma_m)^2 - (\text{Im } \gamma_m)^2}. \qquad \text{(B10)}$$

At each of these special values of β, of which there are infinitely many, Re λ_m assumes, as seen from Eq. (B8), its locally maximum value

$$\max(\text{Re } \lambda_m) = \frac{2\beta}{|\text{Im } \gamma_m^2|} = \frac{\beta}{\text{Re } \gamma_m |\text{Im } \gamma_m|}. \qquad \text{(B11)}$$

We may similarly compute the largest values of Im λ as a function of β. In the plots of Im λ_m versus β for different m, the local maxima are, according to Eq. (B9), approximately located at those values of β that obey the relation

$$\beta^2 = \text{Re } \gamma_m^2 - \text{Im } \gamma_m^2 = (\text{Re } \gamma_m)^2 - (\text{Im } \gamma_m)^2 - 2\text{Re } \gamma_m \text{ Im } \gamma_m. \qquad \text{(B12)}$$

At these β values, Im λ_m attain their maximum magnitudes:

$$\max(\text{Im } \lambda_m) = \frac{\beta}{|\text{Im } \gamma_m^2|} = \frac{\beta}{2|\text{Re } \gamma_m \text{ Im } \gamma_m|}. \qquad \text{(B13)}$$

Note that the maximum values of the real and imaginary parts of λ occur at values of β that are not in general coincident, although, since Re $\gamma_m \approx \beta$ and Im γ_m does not change much through the peak of Eq. (B10), with the help of Eqs. (B11) and (B13) we may write

$$\max(\text{Re } \lambda_m) \approx 2 \times \max(\text{Im } \lambda_m) \approx \frac{1}{|\text{Im } \gamma_m|}. \qquad \text{(B14)}$$

Since for large $|\gamma_m|$ the real part of γ_m dominates its imaginary part, we see from Eqs. (B10) and (B12) that the maximum values of Re λ and Im λ are obtained in the domain where $|\gamma_m| \approx \beta$. As a solution of Eq. (45), let us write

$$\gamma_m = 2m\pi + 2(\epsilon' + i\epsilon''), \qquad \text{(B15)}$$

where m is integral and ϵ' and ϵ'' are real quantities which are of order 1. Then an expansion to the lowest order in ϵ'' of the right-hand side of the first of Eqs. (B5), and use of some simple trigonometric identities, lead to the relation

$$\frac{\tan \epsilon' + i \tanh \epsilon''}{1 - i \tan\epsilon' \tanh \epsilon''} \approx -i \frac{\beta}{2m\pi + 2\epsilon'} - \frac{\epsilon''\beta}{2m^2\pi^2}. \qquad \text{(B16)}$$

Given that the imaginary part dominates the real part on the right in Eq. (B16), we have a variety of possibilities, it would seem, for values of ϵ' and ϵ'' that would lead to consistency with the left side of that equation. In particular, for the largest Re λ for which relation (B10) holds, since the purely imaginary quantity on the right side of Eq. (B16) assumes the value

$$\sqrt{1 - \frac{(\text{Im } \gamma_m)^2}{(\text{Re } \gamma_m)^2}} \approx 1 - \frac{1}{2} \frac{(\text{Im } \gamma_m)^2}{(\text{Re } \gamma_m)^2},$$

it may be shown that consistency with the purely real quantity on the right of Eq. (B16), which is of order $1/\beta$, then

requires that $\tan \epsilon' \approx 1$. With this condition and the preceding equation, the imaginary parts of Eq. (B16) obey the relation

$$-\tanh \text{Im } \gamma_m \approx 1 - \frac{1}{2} \frac{(\text{Im } \gamma_m)^2}{(\text{Re } \gamma_m)^2}. \qquad \text{(B17)}$$

Since the right side is very close to 1, we may replace $-\tanh\text{Im } \gamma_m$ by its asymptotically correct value $1 - 2\exp(-2|\text{Im } \gamma_m|)$. Further, since Re γ_m is close to β, we have the result

$$e^{-|\text{Im } \gamma_m|} = \frac{1}{2\beta} |\text{Im } \gamma_m|. \qquad \text{(B18)}$$

For very large values of β, a convenient form of Eq. (B18) is obtained on taking its logarithm

$$|\text{Im } \gamma_\lambda| = \log 2\beta - \log|\text{Im } \gamma_\lambda|.$$

This relation may be solved for $|\text{Im } \gamma_\lambda|$ iteratively with the following two-term result:

$$|\text{Im } \gamma_\lambda| = \log\left(\frac{2\beta}{\log 2\beta}\right). \qquad \text{(B19)}$$

The largest real and imaginary parts of the eigenvalues now immediately follow from Eq. (B14):

$$\max(\text{Re } \lambda_m) \approx 2 \times \max(\text{Im } \lambda_m) \approx \frac{1}{\log(2\beta/\log 2\beta)}. \qquad \text{(B20)}$$

Similar considerations to these may be used to find the largest real and imaginary parts of the eigenvalues for odd solutions. However, since the distinction between the odd and even solutions becomes small at large mode indices, the final results corresponding to Eq. (B20), but for the odd modes, are nearly the same.

4. Numerical considerations

Our considerations of the eigenvalues have, so far, dealt with approximate analytical expressions for them. Numerical calculations are necessary, however, to compute the eigenvalues with high accuracy, particularly when $|\gamma_\lambda| \sim \beta$. A numerical method that converges rapidly for all values of γ_λ is an iterative one based on the identity

$$\tan^{-1}(iz) = \frac{i}{2}\log\left(\frac{1+z}{1-z}\right). \qquad \text{(B21)}$$

When $|\gamma_\lambda| > \beta$, the solutions to the eigenvalue equation (45) for the even modes may be written conveniently in the form

$$\gamma_m = 2m\pi + 2\epsilon,$$

in which the correction 2ϵ obeys the equation

$$\epsilon = -\tan^{-1}\left(\frac{i\beta}{2m\pi + 2\epsilon}\right).$$

Use of identity (B21) then generates the equation

$$\epsilon = -\frac{i}{2}\log\left(\frac{2m\pi+\beta+2\epsilon}{2m\pi-\beta+2\epsilon}\right), \qquad (B22)$$

in which, on the right-hand side, we initially set ϵ equal to a complex value with small modulus, but then refine its value iteratively by means of the equation.

When $|\gamma_\lambda| < \beta$, the solutions to Eq. (45) are best obtained by first writing it as

$$\cot(\gamma_\lambda/2) = i\frac{\gamma_\lambda}{\beta},$$

and then looking for its solutions of form

$$\gamma_m = (2m+1)\pi + 2\delta.$$

It is straightforward to show that δ obeys an equation analogous to Eq. (B22):

$$\delta = -\frac{i}{2}\log\left|\frac{\beta+(2m+1)\pi+2\delta}{\beta-(2m+1)\pi-2\delta}\right|. \qquad (B23)$$

In much the same way as for ϵ, we could then determine a highly accurate value for δ by a repeated use of Eq. (B23). In most instances, we needed no more than about ten iterations to obtain ϵ and δ—and therefore the root γ_m—to a precision of a part in 10^{10}. A similar procedure can be implemented to solve Eq. (47) efficiently for the roots of the odd modes as well.

APPENDIX C: ASYMPTOTIC EVALUATION OF AN INTEGRAL

The integral

$$F(u) = \frac{2}{\sqrt{\pi}}\int_0^\infty e^{-x^2-16u/x^4}dx \qquad (C1)$$

may be evaluated approximately when u is positive and large. Because the integrand is highly peaked as a function of x, the largest contributions to the integral come from the immediate vicinity of the maximum of the integrand. It is sufficient to carry out, in the integrand, a Taylor expansion of the exponent to the lowest quadratic order around its maximum, which yields

$$e^{-(x^2+16u/x^4)} \approx e^{-3\cdot2^{2/3}u^{1/3}}e^{-6(x-x_0)^2}, \qquad (C2)$$

where x_0, the maximum of the exponent, is equal to $2^{5/6}u^{1/6}$. The neglected third-order term in the exponent depends on u as $1/u^{1/6}$, and so, throughout the range around $x=x_0$ over which the expression (C2) has a value significantly different from zero, a range of order 1, the neglected term is small, provided $u^{1/6} \gg 1$. For such large u values, approximation (C2) represents the integrand quite accurately over that range. To a similar accuracy, we may also extend the limits of integration for the variable $x-x_0$ to $\pm\infty$. The resulting Gaussian integral is a simple one to evaluate, and we obtain

$$F(u) \approx \frac{2}{\sqrt{6}}e^{-3(4u)^{1/3}}. \qquad (C3)$$

[1] R. Wood, *Physical Optics*, 3rd ed. (McMillan, New York, 1934, reprinted by Dover, New York, 1967), p. 597.
[2] L. Biberman, Zh. Éksp. Teor. Fiz. **17**, 416 (1947).
[3] T. Holstein, Phys. Rev. **72**, 1212 (1947); **83**, 1159 (1951).
[4] H. Post, Phys. Rev. A **33**, 2003 (1986).
[5] J. Huennekens and A. Gallagher, Phys. Rev. A **28**, 238 (1983); J. Huennekens, H. Park, T. Colbert, and S. McClain, *ibid.* **35**, 2892 (1987); T. Colbert and J. Huennekens, *ibid.* **41**, 6145 (1990).
[6] M. van Albada, B. van Tiggelen, A. Lagendijk, and A. Tip, Phys. Rev. Lett. **66**, 3132 (1991); G. Watson, P. Fleury, and S. McCall, *ibid.* **58**, 945 (1987).
[7] M. van Albada and A. Lagendijk, Phys. Rev. Lett. **55**, 2692 (1985); P. Wolf and G. Maret, *ibid.* **55**, 2696 (1985); M. van Albada, M. van der Merk, and A. Lagendijk, *ibid.* **58**, 361 (1987).
[8] R. Dicke, Phys. Rev. **93**, 99 (1954).
[9] J. Hopfield, Phys. Rev. **112**, 1555 (1958); C. Kittel, *Quantum Theory of Solids*, 2nd ed. (Wiley, New York, 1987), p. 42; B. Huttner, J. Baumberg, and S. Barnett, Europhys. Lett. **16**, 177 (1991).
[10] D. Burnham and R. Chiao, Phys. Rev. **158**, 667 (1969).
[11] M. Crisp, Phys. Rev. A **1**, 1604 (1970); **5**, 1365 (1972).
[12] S. Prasad and R. Glauber, Phys. Rev. A **31**, 1575 (1985).
[13] N. Skribanowitz, I. Herman, J. MacGillivray, and M. Feld, Phys. Rev. Lett. **30**, 309 (1973); J. MacGillivray and M. Feld, Phys. Rev. A **14**, 1169 (1976); F. Mattar, H. Gibbs, S. McCall, and M. Feld, Phys. Rev. Lett. **46**, 1123 (1981).
[14] R. Glauber, Phys. Lett. **21**, 650 (1966).
[15] J. Jackson, *Classical Electrodynamics*, 2nd ed. (Wiley, New York, 1975), p. 154.
[16] S. Prasad and R. Glauber, Phys. Rev. A **31**, 1583 (1985).
[17] F. Arecchi and E. Courtens, Phys. Rev. A **2**, 1730 (1970).
[18] See, e.g., R. Courant and D. Hilbert, *Methods of Mathematical Physics*, 1st English ed. (Wiley, New York, 1953), Vol. I, Chap. III, Sec. 5.
[19] U. Fano, Phys. Rev. **124**, 1866 (1961).
[20] I. Gradshteyn and I. Ryzhik, *Tables of Integrals, Series, and Products* (Academic Press, 1965), formula 3.325.